# Advanced Pumped Hydro Reverse Osmosis Systems Supplementary Material

Alexander H. Slocum, Maha N. Haji, Zachary Trimble, Marco Ferrara, Sasan J. Ghaemsaidi

31 July 2015
Last edit 07/20/2016

## 1 Introduction to Supplementary Materials

Section 2 describes the first principles analysis used to determine the size maximum salinity output of an APHRO system. Section 3 presents a preliminary geographic potential assessment of various locations around the globe. A detailed economic analysis for the case of an APRHO system in Southern California is presented in Section 4. Section 5 discusses the environmental and cultural considerations that must be taken when developing an APHRO system, while Section 6 discusses the affect of advancements in technology pertaining to renewables and reverse osmosis systems on the total APRHO system cost. Finally, Section 7 describes further research to be done in this area.

## 2 First principles analysis

The system size is a combination of multiple constraints: the volume flow rates are governed by daily requirements for fresh-water, maximum system output salinity, and the cost advantage of inherent renewable energy storage; the renewable energy system is sized to provide the necessary and most cost effective energy based on local conditions per day to the population. The simplified first order analysis presented in this section is used to develop insight into the system sizing and provide reasonable size and cost estimates that can be used by those interested for quick trade studies. A 24-hour period is used where it is assumed that averages of energy, power and fresh water usage and production during this time span are valid estimators. A more detailed analysis is presented later that uses real-time demand and production to provide a more accurate estimate. The first principles analysis is distilled into a spreadsheet that was presented in the previous section and is intended to be used to rapidly evaluate several sites to identify a set of cost effective candidates. Detailed input information should then be obtained for the most promising candidates and a highly detailed analysis (presented later) performed on those candidates to provided accurate economic estimates. Figure 1 depicts the flow of the first principle analysis described in this section.

The ultimate goal of this analysis is to determine the capacity of a renewable energy portfolio that is needed to simultaneously provide a prescribed amount of power and fresh-water.

To begin, the needed volume of fresh water, $V_{fwro}$, is identified. If the volume of fresh-water needed is already known, it can be inputted directly. Otherwise, the total number of people the system is expected to provide water for, $N_{pfw}$, and the expected average water consumption per person per day, $V_{pfw}$, are used to solve for the total volume of fresh water the reverse osmosis system needs to produce each day,

$$V_{fwRO} = V_{pfw} N_{pfw} \tag{1}$$

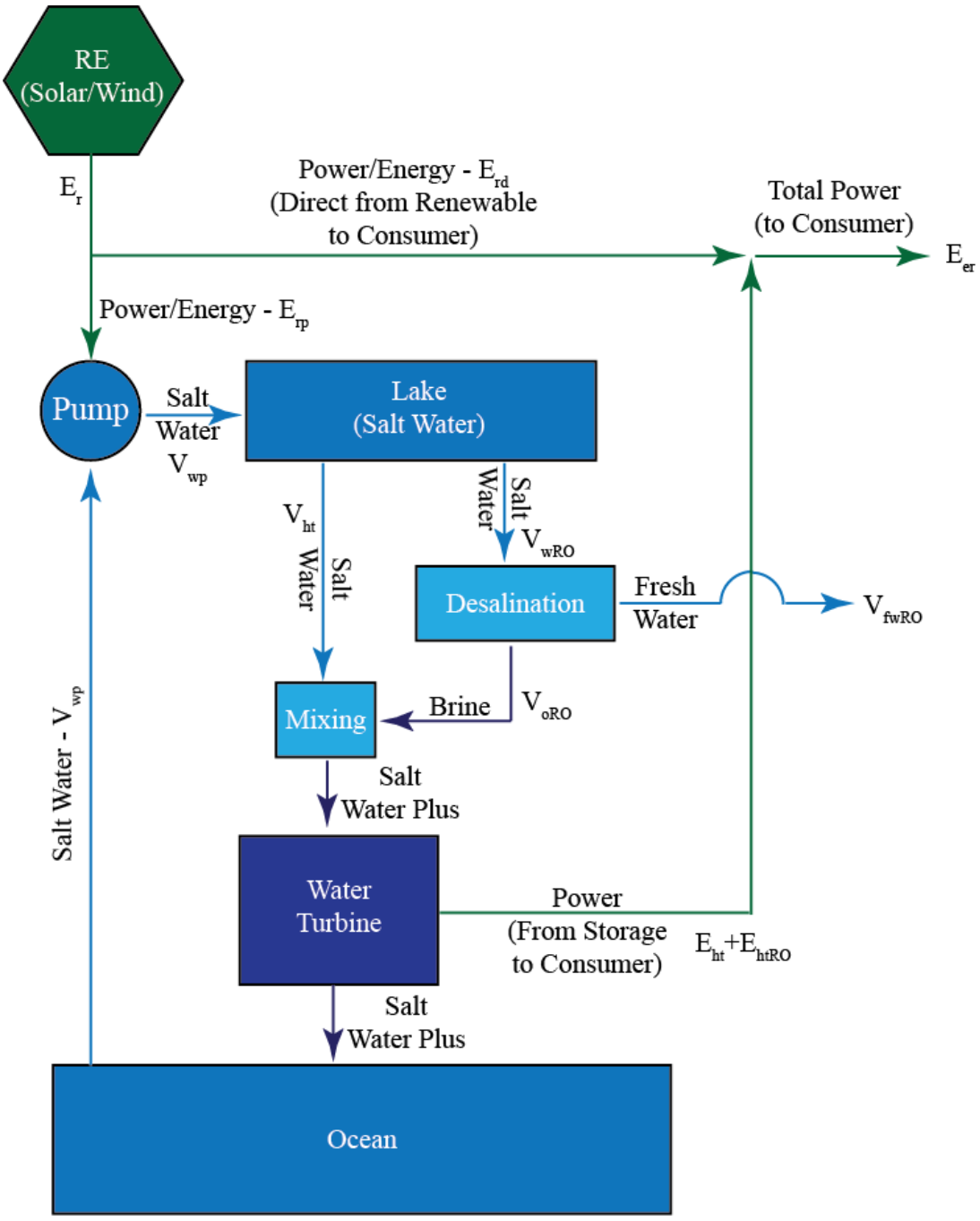


Figure 1: Schematic of flow of first principle analysis for APHROS.

This volume of fresh-water is provided by a reverse osmosis (RO) system that converts some percentage of the input water volume into fresh water. Thus, the total volume of sea-water that must be supplied to the RO plant is,

$$V_{wRO} = \frac{V_{fwRO}}{\eta_{RO}} \tag{2}$$

where $\eta_{RO}$ is the assumed from known references percentage by volume of salt water entering the

RO system that is converted to fresh water. Also exiting the RO system is waste brine water which is still under relatively high pressure. Ideally, this brine water is mixed with the high pressure sea-water flowing from the lake into the power turbine. In reality combining the brine and sea-water steams introduces an efficiency loss whose details are discussed further in the energy section below. Regardless of whether these streams are mixed before or after recovering the energy, mixing the waste brine water from the RO plant with the sea-water flowing to the power turbine reduces the salinity of the brine and thus allows for direct discharge into the ocean. The final output salinity of the system sets a bound on the minimum flow that must be provided to mix with the brine water, $V_{wp_{MIN}}$, to ensure a prescribed maximum output salinity. A mass balance around the RO plant and the mixing of the two streams (details in Appendix 2.1) is used to solve for the minimum total volume of water that must be pumped into the lake each day,

$$V_{wp_{MIN}} = \frac{V_{fwRO}}{\left(1 - \frac{S_{sw}}{S_{ht}}\right)\frac{\rho_{sw}}{\rho_{fw}}} \tag{3}$$

where $S_{sw}$ and $\rho_{sw}$ are the salinity and density of seawater, respectively, $S_{ht}$ is the final output salinity of the system, and $\rho_{fw}$ is the density of fresh-water.

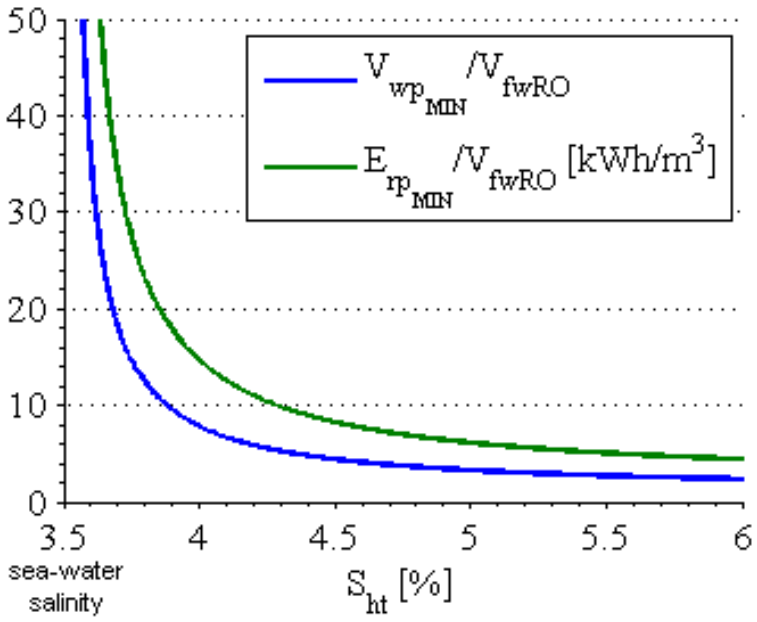


Figure 2: Plot of the ratio of minimum total volume pumped each to day to daily fresh-water output and the minimum energy to pump that total volume of seawater (with $h_L$=600 m; $\eta_{hp}$=0.89) per volume of fresh-water produced both vs the final output salinity.

As seen in Figure 2, the minimum total volume of sea-water that must be pumped per day increases dramatically as the required output salinity approaches that of the sea-water. A final output salinity of 4.3% only requires the total volume to be five times the fresh-water output volume, but reducing the final output salinity to 3.9% doubles the minimum total pumped volume to ten times the fresh water volume. The allowable salinity that can be discharged from the turbine into the sea will depend on local conditions, and the economics must be studied to compare using a diffusing discharge line, which creates more backpressure on the turbine, with simply using much more seawater for generating electricity than for generating freshwater.

Next, the size of the renewable energy system is bounded by the energy requirements of the consumer and the previously solved for fresh water needs. The average energy used per person over a 24-hour period, $E_{p24}$, can be inputted directly, or estimated based on a 24-hour per person power demand, $P_{pe}$, using

$$E_{p24} = 24 * 3600 * P_{pe}. \tag{4}$$

The total energy required for the population served that must be delivered every 24 hours, $E_{er}$, is thus:

$$E_{er} = N_{pe} E_{p24} \tag{5}$$

where $N_{pe}$ is the total number of people whose energy needs are expected to be served by the system. This energy is assumed to be supplied by a renewable energy portfolio but not all of the energy collected by the renewables system can be used by consumers, and it is assumed here a percentage of the renewable resources' power (the excess power) is used by an electric motor to drive a turbine to pump water up to the energy storage reservoir. The gravitational potential energy added to the sea-water is used to supply the RO membranes with pressurized seawater, and when electricity is to be generated to power the turbine in reverse so the motor now acts as a generator. The potential energy of the brine stream exiting the RO system and sea-water stream are $E_{htRO}$ and $E_{ht}$, respectively. renewable energy supplied directly to the consumer by the renewable energy harvest devices is $E_{rd}$. Thus, the total energy supplied to the consumer is the sum of the energy supplied directly and the energy recovered from the brine and sea-water streams,

$$E_{er} = E_{rd} + E_{ht} + E_{htRO}. \tag{6}$$

where the energy supplied directly from the renewable resource to the consumer is,

$$E_{rd} = (1 - \gamma) E_r \tag{7}$$

and the energy supplied by the renewable resource for pumping is,

$$E_{rp} = \gamma E_r \tag{8}$$

where $E_r$ is the daily energy from the renewable source, and $\gamma$ represents the fraction of $E_r$ split between pumping seawater up to the lake and directly supplying the consumer. To determine the total size of the renewable energy system required to supply the water and energy needs of the consumer, each of the terms in (6) must be written in terms of the energy from the renewable source, $E_r$ and known inputs $E_{er}$ and $V_{fwRO}$. Using the factor $\gamma$ the direct supply is already in terms of $E_r$. To write $E_{ht}$ and $E_{htRO}$ in those terms potential energy of a mass of water in the lake is used,

$$E_{L_d} = \eta_T \rho_{sw} V_{wp} g h_L \tag{9}$$

where $E_{L_d}$ is the potential energy of the volume of water pumped to the lake daily, $V_{wp}$ is the volume of the water pumped, and $h_L$ is the height of the lake above seawater. Technically the height $h_L$ is the height of the center of mass of the volume of water being considered, and $\eta_T$ is the round trip efficiency of of the system. The height of this mass of water above the datum is changing as the lake fills and empties. However, the change in lake height is considered small compared to the height of the lake above the ocean, thus a reasonable estimate is to use the elevation of the bottom of the lake. The efficiency terms represent losses in the pump, turbine, piping and reductions in

net head pressure associated with flow. According to [1] existing pumped-hydro energy storage systems have round trip efficiencies exceeding 80%. This total round trip efficiency is broken into efficiency on the pumping side, $\eta_p$, and efficiency on the turbine side, $\eta_{ht}$,

$$\eta_T = \eta_p \eta_{ht}. \tag{10}$$

For initial estimates, losses in the pumping and turbine side are assumed to be equal,

$$\eta_{ht} = \sqrt{\eta_T} = \sqrt{0.8} \approx 0.89. \tag{11}$$

Thus, the total energy that needs to be supplied by the renewable energy system to pump sea-water up into the lake daily is,

$$E_{rp} = \gamma E_r = \frac{E_{L_d}}{\eta_{ht}} = \frac{1}{\eta_{ht}} \rho_{sw} V_{wp} g h_L \Rightarrow E_r = \frac{\rho_{sw} V_{wp} g h_L}{\gamma \eta_{hp}}. \tag{12}$$

Since the user inputs are the energy and water required by the consumer, it makes sense to write this expression in terms of the fresh water needed. First this volume of seawater is split into two streams, one feeding the RO plant and one directly feeding the sea-water turbine that generates electric power,

$$V_{wRO} = \gamma_{RO} V_{wp}, \tag{13}$$

$$V_{ht} = (1 - \gamma_{RO}) V_{wp} \tag{14}$$

where $\gamma_{RO}$ is the percentage of total water pumped to the lake that is later to be input to the RO plant. The seawater feeding the RO plant is further split into two streams one freshwater stream output from the plant which goes to consumers, $V_{fwRO}$[1], and one brine-water stream from which energy is to be recovered before it is discharged into the sea, $V_{oRO}$,

$$V_{fwRO} = \eta_{RO} V_{wRO} = \gamma_{RO} \eta_{RO} V_{wp}, \tag{15}$$

$$V_{oRO} = V_{wRO} - V_{fwRO} = (1 - \eta_{RO}) V_{wRO} = \gamma_{RO} (1 - \eta_{RO}) V_{wp} \tag{16}$$

The energy that can be recovered from the brine stream is dependent on how the streams are combined. To understand how the streams combine, start with an estimate of the efficiency as a function of the various head losses in the system.

The turbine side efficiency represents losses in the turbine and the major and minor losses in the piping network. Thus, the total power that is extracted by the turbine can either be written in terms of the product of the mass flow rate and total head pressure utilizing the turbine side efficiency, or it can be written in terms of the actual head pressure across the turbine where the losses for each element are subtracted from the initial head pressure,

$$P = \eta_{ht} \rho Q g H = \rho g Q \left( H - h_1 - h_t \right). \tag{17}$$

Rearranging, the efficiency can be written as,

$$\eta_{ht} = \frac{H - (h_1 + h_t)}{H}. \tag{18}$$

[1]Depending on the actual pressure and municipal system pressure it might be possible to recover some energy from the fresh water stream as well, but since this is not possible for all systems it is not included in this analysis.

Thus, the turbine side efficiency is the total head of the system minus the head losses normalized by the total head.

An initial thought is to combine the salt water and brine streams into one stream to save on capital cost. However, the brine stream is at a slightly lower head pressure after traveling through the RO plant than the direct salt water stream. To combine these streams directly, the salt water stream would need to go through some sort of head loss that is equivalent to the RO plant head loss. In that case, using the result of eq. 18 the efficiency becomes,

$$\eta_{ht} = \frac{H - (h_1 + h_t + h_{RO})}{H}. \tag{19}$$

The head loss in the RO Plant is assumed to be a known percentage of the inlet pressure to the RO plant,

$$H_{o_{RO}} = \eta_{RO_{io}} H_{i_{RO}} \Rightarrow h_{RO} = (1 - \eta_{RO_{io}})\, H_{i_{RO}} = (1 - \eta_{RO_{io}})\,(H - h_1)\,. \tag{20}$$

Combining these equations results in an expression for the efficiency in terms of the percentage loss in the RO plant,

$$\eta_{ht} = \frac{\eta_{RO_{io}} H - (\eta_{RO_{io}} + h_t)}{H}. \tag{21}$$

Essentially the percentage loss in the RO plant is applied to the system efficiency.

Such a loss will be unacceptable; thus the streams cannot be combined directly before going into a single turbine. At least 3 potential strategies exist: 1. use separate power generating turbines, 2. entrain the brine flow into the salt water flow using the venturi effect, 3. use a multi-stage turbine such that salt water flows into the first stage of the turbine and the head loss from the first stage of the turbine is the same as the head loss in the RO plant so the brine and salt water can be combined and then continue together through the remaining stages of the turbine.

For separate turbines, the sea-water stream has the same efficiency as a stand alone pumped-hydro system and the brine stream's efficiency is scaled by the head loss in the RO plant. Thus, the overall system efficiency is dependent on the flow rate ratios,

$$\eta_{ht_1} = \left[1 - \gamma_{RO} + \eta_{RO_{io}} \gamma_{RO}\,(1 - \eta_{RO})\right] \eta_{ht} \approx 0.87. \tag{22}$$

As shown in the previous flow rate analysis, for the final output salinity to be low the flow rates into the RO Plant are small compared to the total flow rates. For expected flow rates the total efficiency is reduced to about 87%, which is only marginally less than a standard pumped-hydro system. The deterrent to this system is the added capital cost of an additional turbine and the added yearly maintenance cost associated with the added complexity of an additional high salinity turbine for the brine. For some systems the brine flow rate is so small and thus represents such a small percentage of the total energy that an additional turbine is not justified and the energy in the brine would not be utilized (fig. 3) and the brine can simply be combined with the large power turbine output flow and returned to the ocean directly. A final decision requires a more detailed analysis of a specific site.

Entraining the brine flow using a venturi introduces two minor losses into the system, $h_c$ & $h_x$, one for contraction of the salt water flow and one for expansion of the salt water flow. The minor head losses are represented by,

$$h_{c,x} = K_{c,x} \frac{\bar{U}_{c,x}^2}{2g} \approx K_{c,x} \frac{Q_{wp}^2}{2gA^2}. \tag{23}$$

Utilizing the total volume of water pumped, $Q_{wp}$, to estimate the average flow velocity is a conservative estimate since the actual flow rate is reduced by the amount of fresh water generated. The $K$ factors are functions of the area ratio which is in turn a function of the flow rates and pressure drop required to entrain the flow. However, since the $K$ factors have a maximum value of 1 assuming such represents a conservative estimate. Thus, the total efficiency is given as,

$$\eta_{ht_2} = \frac{H - (h_1 + h_e + h_t)}{H} \approx 87\%. \tag{24}$$

Since the system operates in the fairly constant region of the Colbrook friction factor estimation this estimate is stable over a wide range or realistic pipe diameters and flow rates, thus an entrainment system is expected to reduce the overall efficiency at most from 89% to 87%.

A multi-stage turbine system will have similar efficiencies as that of the individual turbines case. Again the question here is one of capital cost and complexity. The best choice is part of a specific site analysis, but for the first principle analysis it is sufficient to know that in all three systems have approximately the same worst case efficiency of about 87%.

Since each of the mixing strategies results in the same overall efficiency, any of the strategies can be used to proceed with the energy analysis and the result will be the same. The most straight forward strategy to use is the two turbine strategy. In that case, the energy from the brine stream is,

$$\begin{aligned} E_{htRO} &= V_{oRO}\rho_{oRO}g\eta_{ROio}h_L\eta_{ht} && (25)\\ &= \gamma_{RO}(1-\eta_{RO})V_{wp}\rho_{oRO}g\eta_{ROio}h_L\eta_{ht} && (26)\\ &= \gamma_{RO}\left(1-\eta_{RO}\frac{\rho_{fw}}{\rho_{sw}}\right)\eta_{ROio}\eta_{hp}\eta_{ht}\gamma E_r. && (27)\end{aligned}$$

Similarly, the energy recovered from the water flowing directly to the turbine from the lake is,

$$\begin{aligned} E_{ht} &= V_{ht}\rho_{sw}gh_L\eta_{ht} && (28)\\ &= (1-\gamma_{RO})\,V_{wp}\rho_{sw}gh_L\eta_{ht} && (29)\\ &= (1-\gamma_{RO})\,\eta_{hp}\eta_{ht}\gamma E_r. && (30)\end{aligned}$$

Combining Equations (6), (27), and (30) and solving simultaneously with Equation (15) yields a solution for $E_r$ in terms of the consumer energy, $E_{er}$, and the freshwater, $V_{fwRO}$, needs and the properties of the pumped hydro system,

$$E_r = E_{er} + \frac{V_{fwRO}\rho_{sw}gh_L}{\eta_{hp}\eta_{RO}\gamma_{RO}}\left[1-\eta_{hp}\eta_{ht}\left(1+\gamma_{RO}-\gamma_{RO}\eta_{ROio}+\eta_{RO}\eta_{ROio}\gamma_{RO}\frac{\rho_{fw}}{\rho_{sw}}\right)\right] \tag{31}$$

The ratio of power available in the brine output of the RO plant to power available from the salt-water flowing directly from the lake to the turbine is,

$$\frac{E_{htRO}}{E_{ht}} = \frac{\gamma_{RO}\left(1-\eta_{RO}\frac{\rho_{fw}}{\rho_{sw}}\right)}{1-\gamma_{RO}}. \tag{32}$$

Figure 3 demonstrates the affect of the percentage of total water volume flowing to the RO plant on the ratio of energy recovered from the brine stream. The total capacity of the renewable energy system is estimated by assuming the above energy is obtained by a constant power input over the 24-hour period.

$$P_r = \frac{E_r}{24 \times 3600} \tag{33}$$

## 2.1 Detailed Calculations of Salinity and Density of the mixed streams

### 2.1.1 RO plant

For this analysis, the RO Plant is modeled as a black box. Shown in Figure 4, salt water from the lake with salinity $S_{sw}$ and density $\rho_{sw}$ is the only input to the plant, and fresh water with zero salinity $S_{fw} = 0$ and density $\rho_{fw}$ and brine with salinity $S_{oRO}$ and density $\rho_{oRO}$ are the outputs from the plant.

It is assumed that the volumetric fresh water output is some percentage of the salt water input,

$$V_{fwRO} = \eta_{RO} V_{wRO}. \tag{34}$$

It is reasonable to assume that the the fluid streams are incompressible and thus the brine volume is,

$$V_{wRO} = V_{fwRO} + V_{oRO} \Rightarrow V_{oRO} = (1 - \eta_{RO})\, V_{wRO}. \tag{35}$$

Although the sea water coming into the RO plant is a complicated combination of many things, for this simplified analysis the seawater is modeled as only a combination of freshwater and salt. Consequently, the brine is also modeled as only salt and fresh water. Under these assumption, a mass balance of fresh-water and a mass balance of salt flowing through the plant is used to calculate the salinity and density of the brine stream. The mass balance of salt flowing through the system is,

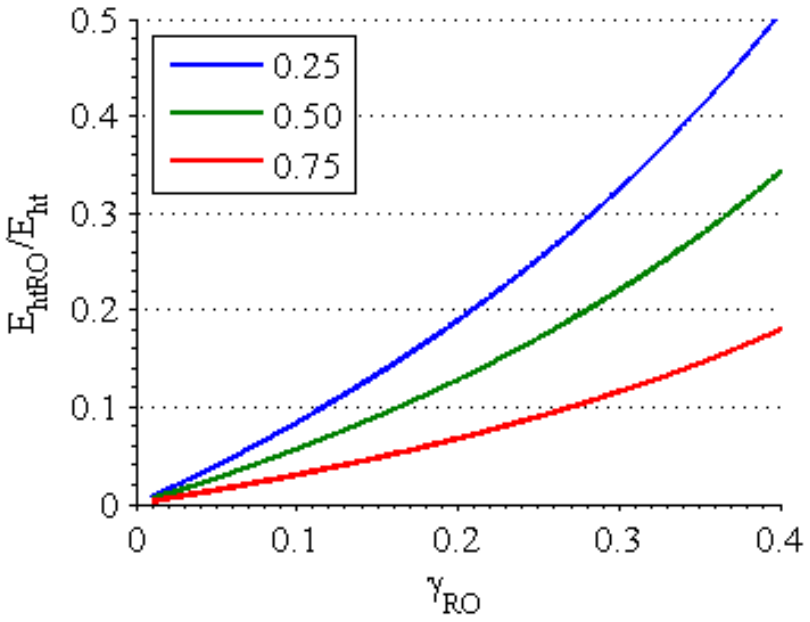


Figure 3: Ratio of energy recovered from the brine stream to energy recovered from the salt water flowing directly from the lake as a function of the percentage of the total water volume flowing to the RO plant for three different conversion ratios $\eta_{RO}$.

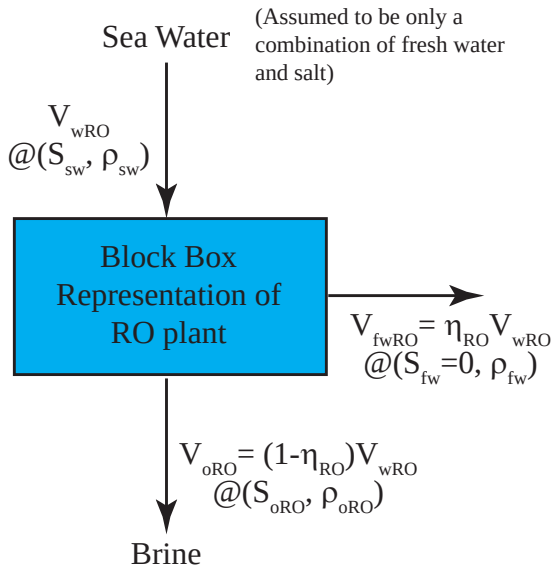


Figure 4: Black box representation of RO plant

$$\dot{m}_{sw_{in}} = \dot{m}_{sw_{out}} \tag{36}$$
$$S_{sw}\rho_{sw}\dot{V}_{wRO} = S_{oRO}\rho_{oRO}\dot{V}_{oRO} = S_{oRO}\rho_{oRO}\left(1-\eta_{RO}\right)\dot{V}_{wRO} \tag{37}$$
$$S_{sw}\rho_{sw} = S_{oRO}\rho_{oRO}\left(1-\eta_{RO}\right), \tag{38}$$

and the mass balance of fresh water through the system is,

$$\dot{m}_{fw_{in}} = \dot{m}_{fw_{out}} \tag{39}$$
$$\left(1-S_{sw}\right)\dot{V}_{wRO}\rho_{sw} = \rho_{fw}\dot{V}_{fwRO} + \left(1-S_{oRO}\right)\rho_{oRO}\dot{V}_{oRO} \tag{40}$$
$$\left(1-S_{sw}\right)\dot{V}_{wRO}\rho_{sw} = \rho_{fw}\eta_{RO}\dot{V}_{wRO} + \left(1-S_{oRO}\right)\rho_{oRO}\left(1-\eta_{RO}\right)\dot{V}_{wRO} \tag{41}$$
$$\left(1-S_{sw}\right)\rho_{sw} = \rho_{fw}\eta_{RO} + \left(1-S_{oRO}\right)\rho_{oRO}\left(1-\eta_{RO}\right) \tag{42}$$

These equations can be solved simultaneously for both salinity and density,

$$S_{oRO} = \frac{\rho_{sw}}{\rho_{sw}-\eta_{RO}\rho_{fw}}S_{sw} \tag{43}$$
$$\rho_{oRO} = \frac{1-\eta_{RO}\frac{\rho_{fw}}{\rho_{sw}}}{1-\eta_{RO}}\rho_{sw} \tag{44}$$

### 2.1.2 Mixing of Brine and Salt Water

Similarly, the the mixing of the brine stream and the salt water from the lake is modeled as a black box, detailed in Figure 5.

Hence, the salt mass balance is,

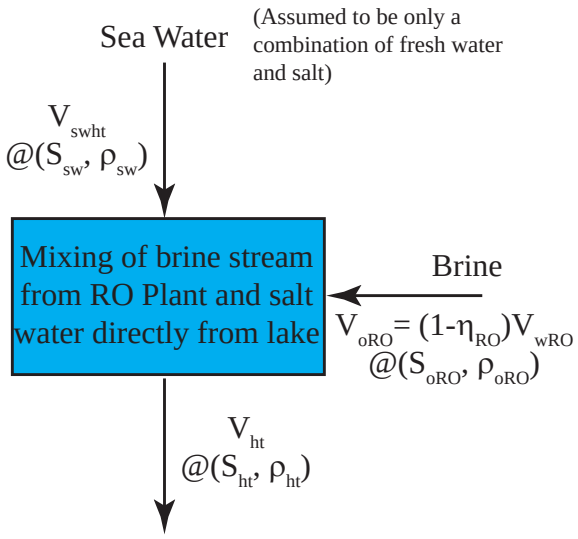


Figure 5: Black box representation of mixing the salt water directly from the lake with the brine stream from the RO plant.

$$\rho_{sw}\dot{V}_{swht}S_{sw} + \rho_{oRO}\dot{V}_{oRO}S_{oRO} = \rho_{ht}\dot{V}_{ht}S_{ht} \tag{45}$$

$$\rho_{sw}\left(\frac{1-\gamma_{RO}}{\gamma_{RO}}\right)S_{sw} + \frac{\eta_{RO}}{1-\eta_{RO}}\left(\rho_{sw}-\rho_{fw}\right)\left(1-\eta_{RO}\right)\left(\frac{\rho_{sw}}{\rho_{sw}-\rho_{fw}}\right)S_{sw} = \rho_{ht}\left[\left(\frac{1-\gamma_{RO}}{\gamma_{RO}}\right)+\left(1-\eta_{RO}\right)\right]S_{ht} \tag{46}$$

The freshwater mass balance is,

$$\rho_{sw}\dot{V}_{swht}\left(1-S_{sw}\right) + \rho_{oRO}\dot{V}_{oRO}\left(1-S_{oRO}\right) = \rho_{ht}\dot{V}_{ht}\left(1-S_{ht}\right) \tag{47}$$

$$\rho_{sw}\left(\frac{1-\gamma_{RO}}{\gamma_{RO}}\right)\left(1-S_{sw}\right) + \frac{\eta_{RO}}{1-\eta_{RO}}\left(\rho_{sw}-\rho_{fw}\right)\left(1-\eta_{RO}\right)\left(1-\frac{\rho_{sw}}{\rho_{sw}-\rho_{fw}}S_{sw}\right) = \rho_{ht}\left[\left(\frac{1-\gamma_{RO}}{\gamma_{RO}}\right)+\left(1-\eta_{RO}\right)\right]\left(1-S_{ht}\right) \tag{48}$$

Solving the system of equations yields the final salinity and density of water that is dumped back into the ocean,

$$S_{ht} = \frac{\rho_{sw}}{\rho_{sw}-\gamma_{RO}\eta_{RO}\rho_{fw}}S_{sw} \tag{49}$$

$$\rho_{ht} = \frac{1-\gamma_{RO}\eta_{RO}\frac{\rho_{fw}}{\rho_{sw}}}{1-\gamma_{RO}\eta_{RO}}\rho_{sw} \tag{50}$$

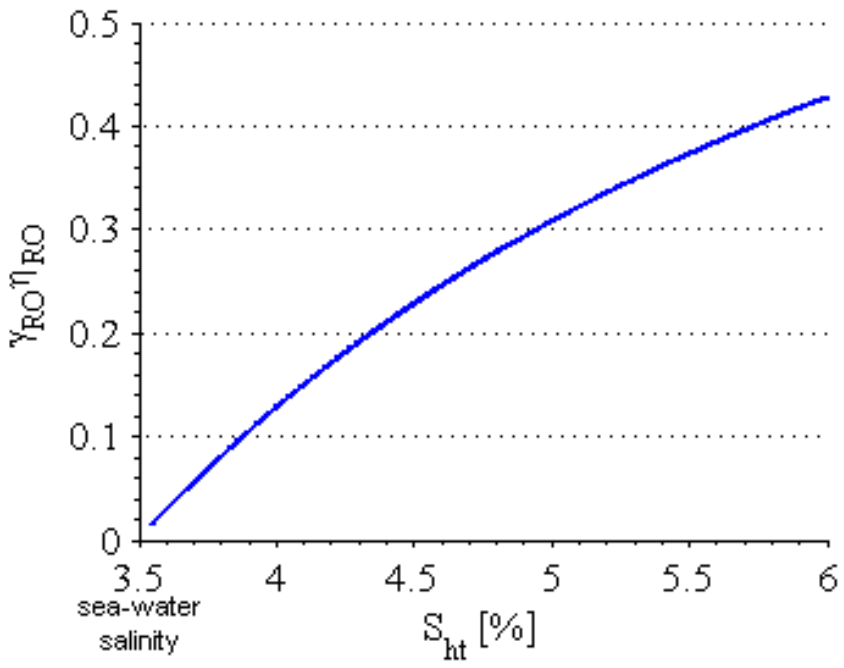


Figure 6: Maximum product of $\gamma_{RO}\eta_{RO}$ to ensure a final output salinity. For example, if the maximum salinity of the output stream is 4% then $\gamma_{RO}\eta_{RO}$ must be less than or equal to 0.13. Thus, if the RO plant is assume to convert 50% of its input volume to fresh water ($\eta_{RO} = 0.5$) then the maximum percentage of pumped sea-water that can be sent to the RO plant is $\gamma_{RO} \leq 0.26$.

## 3 Additional Locations

This section details the geographic potential assessment of the following regions:

- Southern California
- Baja California
- Hawaii
- Peru
- Chile
- Brazil
- Morocco
- Northern Red Sea (Egypt, Israel, and Jordan)
- Iran
- UAE
- China (East)

Although some of these locations are also presented in the article they are reproduced here for completeness. As such, all locations that have thus far been analyzed are presented in one coherent location for comparison.

## 3.1 Southern California

Southern California is very dry with a very large population, and takes water from the Owen's valley, so if this water was no longer needed, farming in the valley might flourish [2, 3, 4]. In southern California, the mountains around Malibu and San Clemente have great promise for IPHRO systems as shown in Figures 7 and 8.

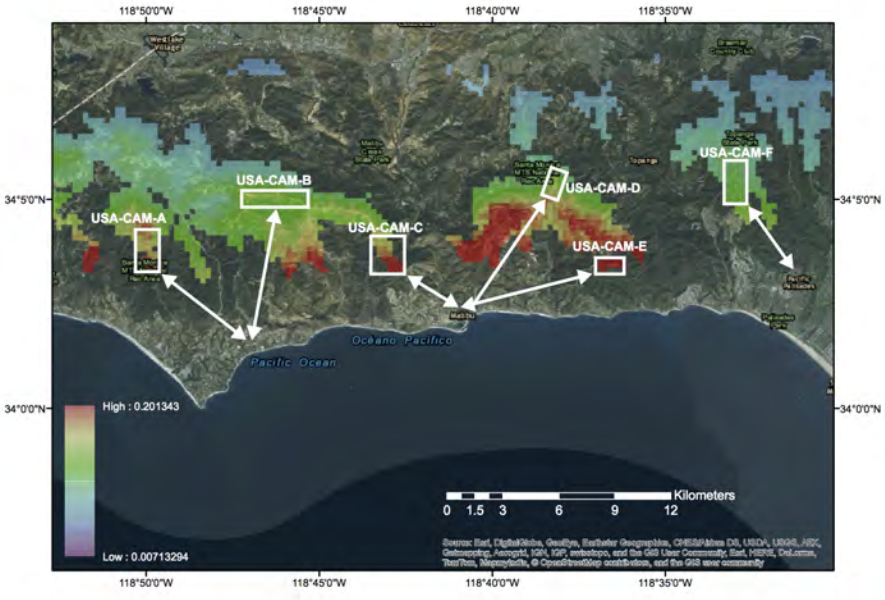


Figure 7: A-Index for topography near Malibu, California. Regions for potential APRHOS applications highlighted in white with distance to nearest major city, Malibu and Pacific Palisades in the case of region USA-CAM-F, indicated by arrows.

Based on the resulting qualitative A-Index (good mountain height within tunneling distance from shore) for areas around Malibu and San Clemente, regions highlighted were selected for further analysis (Figs. 7 and 8). These regions have a total upper reservoir (lake) area potential of approximately 14.7 km$^2$. Assuming these are all developed into APRHOS lakes in which 30 m of water is pumped up and down with each cycle, these regions could provide power and freshwater for about 28 million people. A reservoir depth of 30 m is considered reasonable because it is a depth easily reached by divers if any maintenance is needed, although a smaller area or more people served could be realized with greater depth of draw. As shown in Figure **??** the amount of seawater needed for desalination is only 4.7% of the total pumped to the lake. If the priority is for more freshwater for piping to interior regions, freshwater for 236 million people could readily be provided by diverting about 37% of the flow to the RO system. This was determined using the minimum allowable turbine diversion to the brine outflow, an ambient seawater salinity of $S_{sw} = 3.5\%$, a desired brine outflow salinity of no more than $S_{ht} = 4\%$ (in keeping with California guidelines and

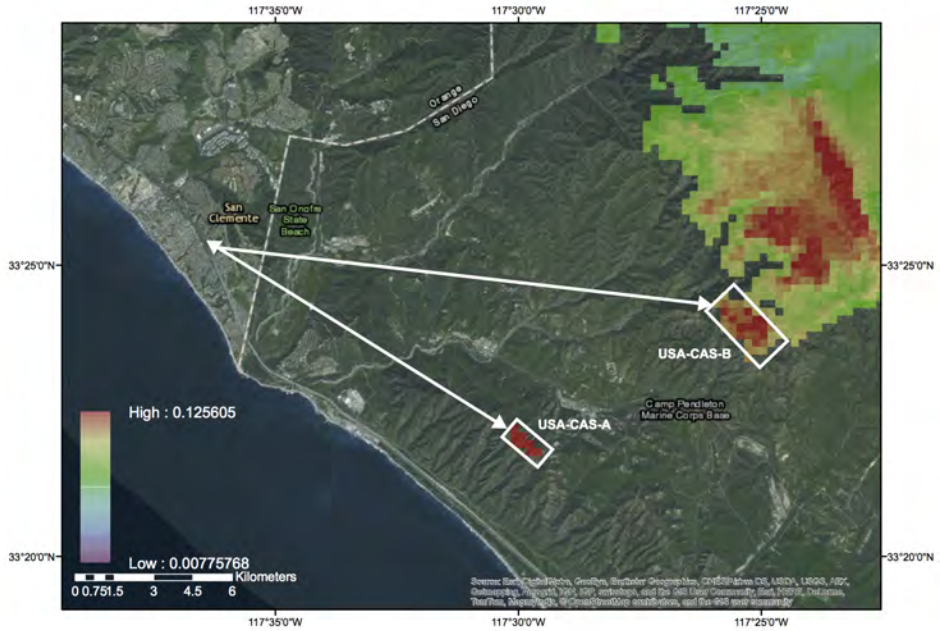


Figure 8: A-Index for topography near San Clemente, California. Regions for potential APRHOS applications highlighted in white with distance to nearest major city, San Clemente, indicated by arrows.

regulations [5]), a seawater density of $\rho_{sw} = 1027$ kg/m$^3$, and a freshwater density of $\rho_{fw} = 1000$ kg/m$^3$. Details are provided in the supplementary materials. By comparison, the population of Malibu and San Clemente are 12,645 and 63,522 respectively, while the Greater Los Angeles region is 18.55 million [6].

Table 1: Energy potential of APRHOS in regions surrounding in Southern California

| **Region** | **Head (m)** | **Surface area (km$^2$)** | **Distance from coast (km)** | **A-Index** | **Nearest major city (NMC)** | **Distance to to NMC** | **Energy potential (GWh/cycle)** |
|---|---|---|---|---|---|---|---|
| USA-CAM-A | 612 | 2.9 | 5.2 | 0.112 | Malibu | 5.9 | 119 |
| USA-CAM-B | 684 | 2.2 | 7.7 | 0.089 | Malibu | 8.8 | 101 |
| USA-CAM-C | 528 | 1.7 | 4.3 | 0.123 | Malibu | 3.3 | 59 |
| USA-CAM-D | 678 | 0.9 | 6.9 | 0.098 | Malibu | 8 | 42 |
| USA-CAM-E | 518 | 1.3 | 2.7 | 0.192 | Malibu | 8 | 44 |
| USA-CAM-F | 545 | 2.4 | 7.2 | 0.076 | Pacific Palisades | 7.9 | 89 |
| USA-CAS-A | 505 | 0.5 | 4.1 | 0.123 | San Clemente | 14 | 17 |
| USA-CAS-B | 552 | 2.8 | 13.3 | 0.042 | San Clemente | 20 | 104 |

## 3.2 Baja California

The cities of Ensenada and Tijuana, 84 km to the north, have a combined population of 1.77 million [7]. The mountains around Ensenada are well-suited for an IPHRO system as shown in Figures 9 and 10.

Following a similar analysis to that done for southern California, regions selected for further analysis are highlighted in Figures 9 and 10 and detailed in Tables 1 and 2 respectively. These regions represent a total lake area of approximately 31.3 km$^2$ and could provide power and freshwater

for about 28.8 million people; hence significant water export, perhaps via a pipeline to Southern California, could be realized.

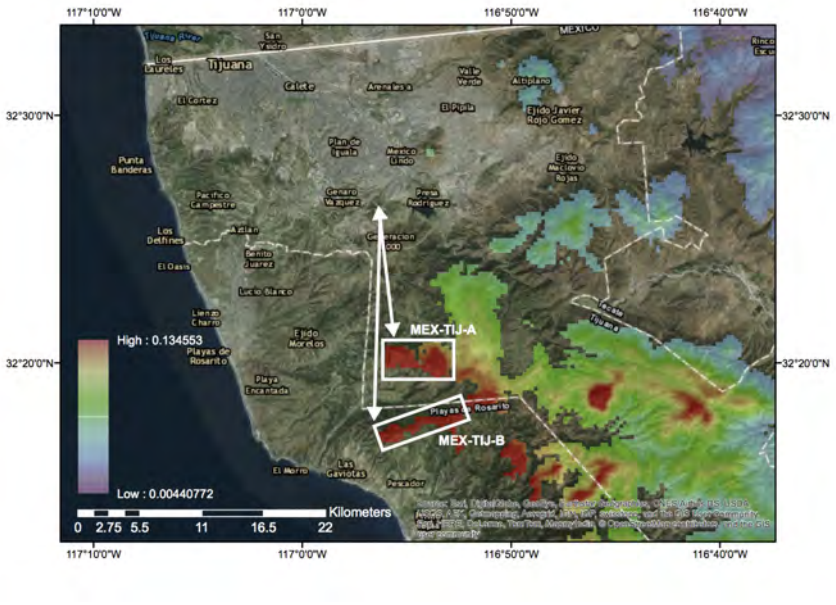


Figure 9: A-Index for topography near Tijuana, Mexico in Baja California. Regions for potential APRHOS applications highlighted in white with distance to nearest major city, Tijuana, indicated by arrows.

Table 2: Energy potential of APRHOS in regions in Baja California, Mexico

| **Region** | **Head (m)** | **Surface area (km$^2$)** | **Distance from coast (km)** | **A-Index** | **Nearest major city (NMC)** | **Distance to to NMC** | **Energy potential (GWh/cycle)** |
|---|---|---|---|---|---|---|---|
| MEX-ENS-A | 886 | 3.5 | 15 | 0.059 | Ensenada | 9.2 | 119 |
| MEX-ENS-B | 636 | 2.7 | 9.6 | 0.066 | Ensenada | 7.6 | 101 |
| MEX-TIJ-A | 567 | 14.5 | 12.7 | 0.045 | Tijuana | 12.8 | 483 |
| MEX-TIJ-B | 542 | 10.7 | 8.2 | 0.066 | Tijuana | 18.8 | 388 |

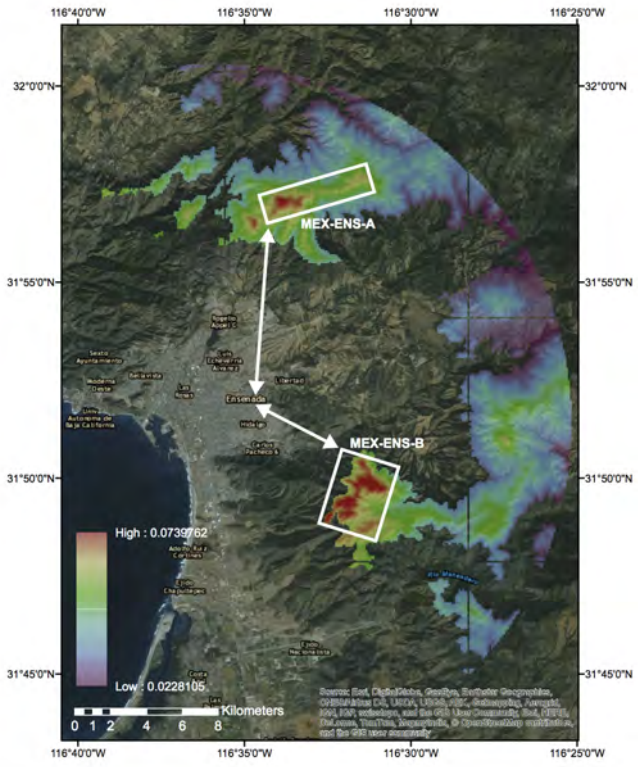


Figure 10: A-Index for topography near Ensenada, Mexico in Baja California. Regions for potential APRHOS applications highlighted in white with distance to nearest major city, Ensenada, indicated by arrows.

### 3.3 Hawaii

Lanai in particular is well suited to an IPHRO system because the population is small but in great need of freshwater and electricity. In addition, single private ownership of most of the island and the desire to develop the island's resort potential could enable rapid responsible development of an IPHRO system which would then serve as a powerful learning project for the other islands. Figure 11 depicts the resulting A-Index for the island and highlights regions further detailed in Table 3. From this analysis, it can be seen that the highlighted regions represent a total lake area of approximately 5.8 $km^2$, which, if developed for IPHROS, could provide power and electricity for nearly 5.4 million people. With a population of only 3,102 [6], by Figure **??** only about 3366 $m^2$ of this total lake area must be developed into IPHROS in order to provide the entire island with power and freshwater.

More populated than Lanai, the island of Maui also faces significant electricity and freshwater demand challenges. The resulting A-Index for the island is shown in Figure 12 with these areas detailed further in Table 3. The total highlighted regions have a combined lake area of $16.5^2$, which represent power and electricity for 15.2 million people. As in the case of Lanai, the population of Maui is much smaller than the total population potential that could served by all possible IPHROS installations on the island. In fact, to serve the entire population of 144,444 [6], would only require

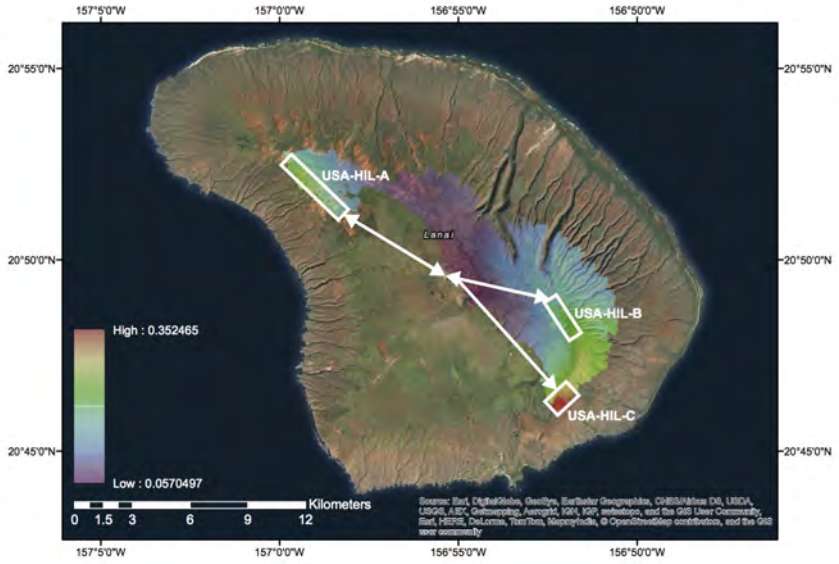


Figure 11: A-Index for topography of the island of Lanai, Hawaii. Regions for potential APRHOS applications highlighted in white with distance to nearest major city indicated by arrows.

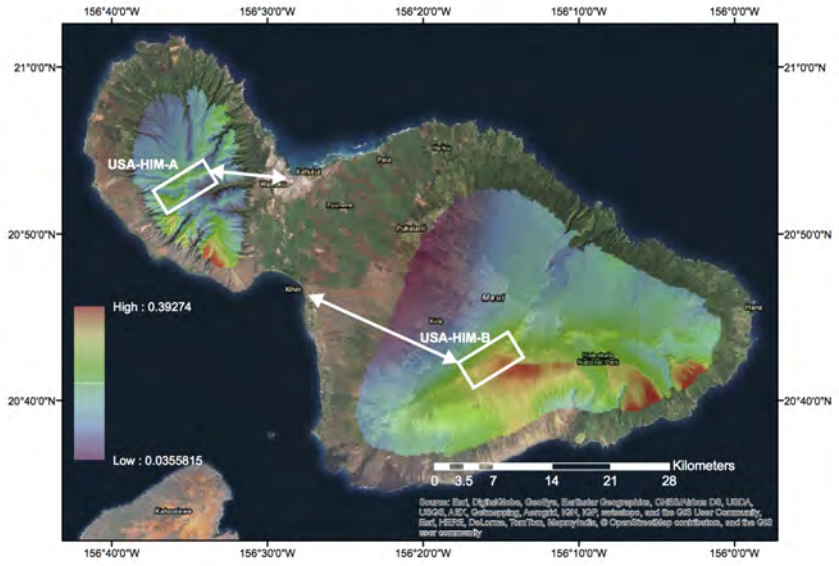


Figure 12: A-Index for topography of the island of Maui, Hawaii. Regions for potential APRHOS applications highlighted in white with distance to nearest major city indicated by arrows.

an IPHROS system with a lake area of 0.16 km$^2$. In fact, the existing Auwahi Wind site located on the wind-rich Ulupalakua Ranch on the southeast coast of Maui, is at an elevation with a high

A-index. An IPHRO system could thus be added to the wind farm to provide needed energy storage and freshwater for the Hawaiian owned farms in the region which are in great need of freshwater for irrigation.

The most populated of the Hawaiian islands, Oahu is faced with even greater electricity and freshwater challenges than Lanai and Maui. The A-Index resulting from geographical analysis of the island are depicted in Figure 13. Regions highlighted in white were selected for further investigation and the details of the IPHROS viability are listed in Table 3. From this data, there exits approximately 20 km$^2$ that could be developed into IPHROS, providing electricity and power for 18.5 million people. With the population of Oahu about 953,207 [6], only a little over 1 km$^2$ is required to meet the energy and water needs of the resident population.


Figure 13: A-Index for topography of the island of Oahu, Hawaii. Regions for potential APRHOS applications highlighted in white with distance to nearest major city indicated by arrows.

Table 3: Energy potential of APRHOS in regions in Hawaii

| **Region** | **Head (m)** | **Surface area (km$^2$)** | **Distance from coast (km)** | **A-Index** | **Nearest major city (NMC)** | **Distance to to NMC** | **Energy potential (GWh/cycle)** |
|---|---|---|---|---|---|---|---|
| USA-HIL-A | 516 | 2.3 | 3.3 | 0.157 | Lanai City | 6.6 | 103 |
| USA-HIL-B | 953 | 1.2 | 6.0 | 0.159 | Lanai City | 5.0 | 80 |
| USA-HIL-C | 552 | 1.6 | 2.1 | 0.268 | Lanai City | 8.6 | 59 |
| USA-HIM-A | 1300 | 5.9 | 7.5 | 0.173 | Kahului | 7.6 | 515 |
| USA-HIM-B | 2757 | 11 | 11 | 0.257 | Kihei | 21 | 1963 |
| USA-HIO-A | 1192 | 0.65 | 8.5 | 0.140 | Mililani Town | 14 | 52 |
| USA-HIO-B | 650 | 5.5 | 4.4 | 0.148 | Honolulu | 12 | 238 |
| USA-HIO-C | 714 | 2.2 | 7.2 | 0.099 | Honolulu | 7.5 | 106 |

## 3.4 Peru

The region around the city of Lima holds great promise for IPHRO systems. Figure 14 shows an image of the region and the potential lake area. With a population of nearly 8.5 million people, if all the highlighted regions were developed for IPHROS, they could provide enough power and water for 87 million people. Therefore, only 10% need to be developed to serve the entire population of Lima. Highlighted regions are further detailed in Table 4.

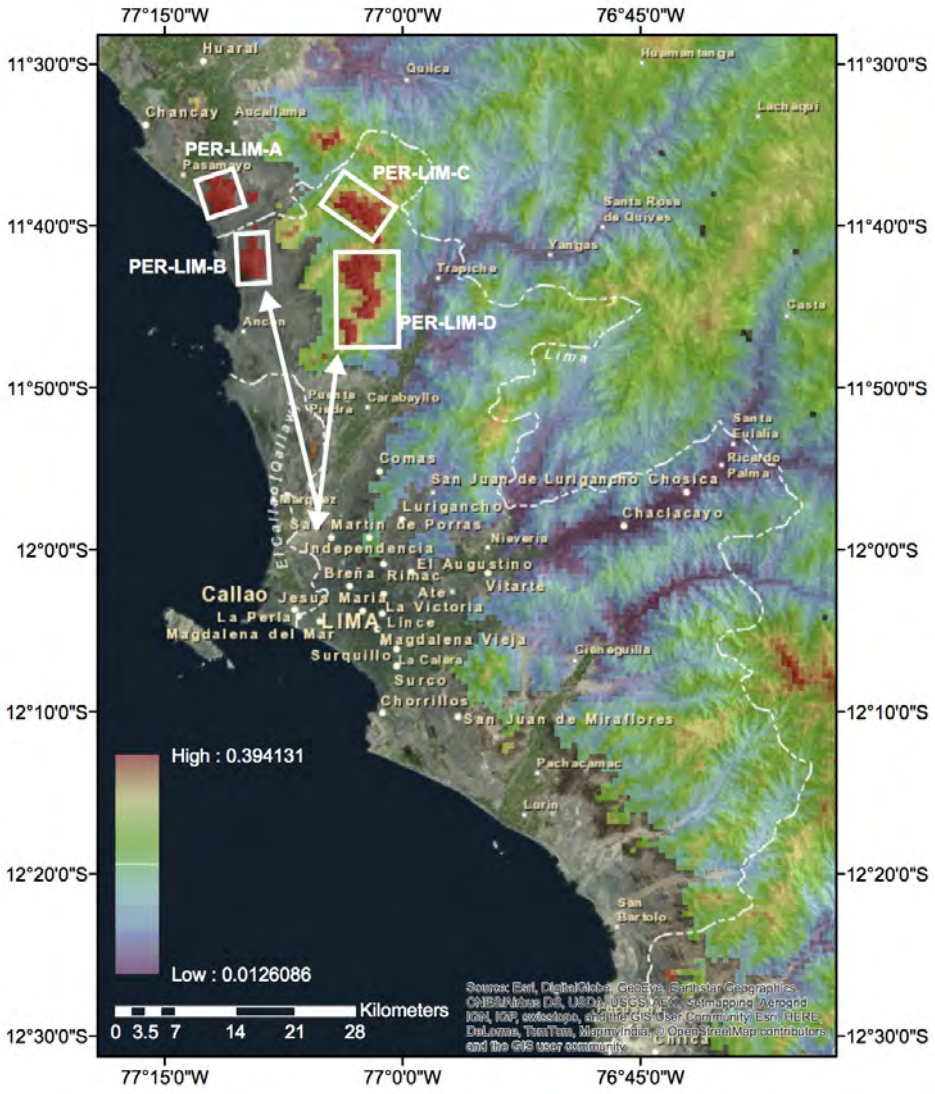


Figure 14: A-Index for topography near Lima, Peru. Regions for potential APRHOS applications highlighted in white with distance to nearest major city, Lima, indicated by arrows.

Table 4: Energy potential of APRHOS in regions in Peru

| Region | Head (m) | Surface area (km$^2$) | Distance from coast (km) | A-Index | Nearest major city (NMC) | Distance to to NMC | Energy potential (GWh/cycle) |
|---|---|---|---|---|---|---|---|
| PER-LIM-A | 592 | 17 | 2.9 | 0.203 | Lima | 38.5 | 704 |
| PER-LIM-B | 574 | 16 | 3.2 | 0.179 | Lima | 30.5 | 627 |
| PER-LIM-C | 1339 | 25 | 1.6 | 0.078 | Lima | 31 | 2214 |
| PER-LIM-D | 1184 | 36 | 14 | 0.083 | Lima | 20.5 | 2854 |

## 3.5 Chile

In Northern Chile, the city of Iquique lies on the Pacific ocean and at the base of a high plateau which makes it an ideal site for an IPHRO system as the region is very dry. Figure 15 shows an image of the region and the potential lake area. Valhalla Energy already has done nearby site engineering and obtained approval for a pumped hydro energy system approximately 98 km south of Iquequi[2], and thus this site could perhaps be the best first application for the IPHRO system anywhere in the world simply because a seawater pumped hydro and renewable energy system is already being planned. Indeed, other water starved regions around the world with IPHRO potential may want to invest in this early project as a means of also gaining rapid insight into the project and the process by which it is executed.

Again, regions selected for further analysis are highlighted in Figure 15 and detailed in Table 5. These regions represent a total lake area of approximately 24.3 km$^2$ and could provide power and freshwater for about 22.4 million people. Given that the population of Iquique is only 180,601 [8], this "extra" water could be used to develop farms in the high desert, or for mining operations.

Table 5: Energy potential of APRHOS in regions in Chile

| Region | Head (m) | Surface area (km$^2$) | Distance from coast (km) | A-Index | Nearest major city (NMC) | Distance to to NMC | Energy potential (GWh/cycle) |
|---|---|---|---|---|---|---|---|
| CHL-IQU-A | 738 | 9.9 | 1.3 | 0.572 | Iquique | 7.4 | 483 |
| CHL-IQU-B | 981 | 9.4 | 7.2 | 0.136 | Iquique | 9.0 | 388 |
| CHL-IQU-C | 586 | 1.2 | 1.6 | 0366 | Iquique | 3.0 | 208 |
| CHL-IQU-D | 893 | 3.9 | 2.3 | 0.388 | Iquique | 9.5 | 113 |

## 3.6 Brazil

With populations of 21.1 million and 12 million , respectively, the cities of São Paulo and Rio de Janeiro in Brazil are some of the most populated in the world [9]. Situated between the Brazilian Highlands and the coast of the Atlantic Ocean, these areas lend themselves to adoption of APHROS for power and freshwater needs, as shown in Figures 16 and 17.

Table 6 describes the characteristics of the regions highlighted in Figures 16 and 17 for further analysis. They represented a combined lake area of 642 km$^2$, which could provide power and freshwater for about 591 million people, far greater than the combined population of the regions themselves. While some coastal regions themselves may not require large volumes of freshwater, nearby regions have low rainfall [10] and thus could greatly benefit. Furthermore, with rapidly changing climate precipitated by deforestation, there may soon be a greater need for freshwater in the region. Nevertheless, Brazil's wind power and solar potential are great, and pumped hydro storage can help to catalyze full development with the added potential benefit of massive freshwater production potential. This could also help to shift hydropower focus from the Amazon where environmental effects of damming rivers is of great concern.

[2]See `http://valhalla.cl/en/espejo-de-tarapaca/`

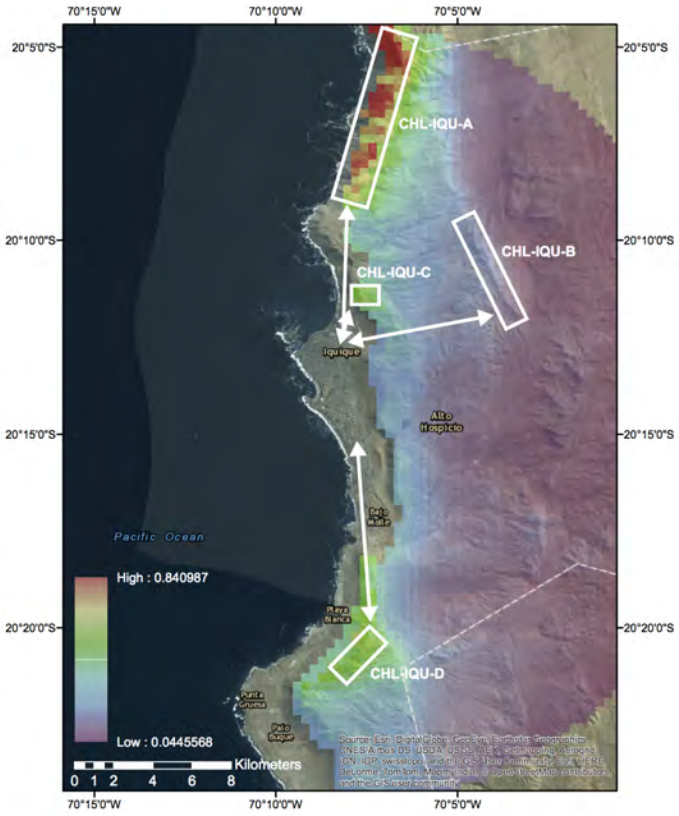


Figure 15: A-Index for topography near Iquique, Chile. Regions for potential APRHOS applications highlighted in white with distance to nearest major city, Iquique, indicated by arrows.

Table 6: Energy potential of APRHOS in regions in Brazil

| **Region** | **Head (m)** | **Surface area (km$^2$)** | **Distance from coast (km)** | **A-Index** | **Nearest major city (NMC)** | **Distance to to NMC** | **Energy potential (GWh/cycle)** |
|---|---|---|---|---|---|---|---|
| BRZ-SAO-A | 770 | 176 | 15 | 0.050 | São Paulo | 82 | 9085 |
| BRZ-SAO-B | 826 | 109 | 9.7 | 0.085 | São Paulo | 34 | 6047 |
| BRZ-SAO-C | 595 | 139 | 4.8 | 0.124 | São Paulo | 74 | 5535 |
| BRZ-RIO-A | 727 | 74 | 4.8 | 0.151 | Rio de Janeiro | 16 | 3602 |
| BRZ-RIO-B | 638 | 52 | 11 | 0.058 | Rio de Janeiro | 1.2 | 2242 |
| BRZ-RIO-C | 617 | 56 | 5.5 | 0.112 | Rio de Janeiro | 0.78 | 2332 |
| BRZ-RIO-D | 600 | 37 | 10 | 0.060 | Rio de Janeiro | 27 | 1477 |

## 3.7 Morocco

The country of Morocco, also pressed with freshwater challenges, has great APHROS potential. Figure 18 highlights regions around the city of Agadir and Guolimim that have particularly high A-Indices. The regions highlighted in white were further investigated with the details of the APHROS analysis listed in Table 7. There are approximately 292 km$^2$ in the mountains around the city of Agadir that could be developed into APRHOS. This resulting freshwater could be sent by canal to the east and south for the parched regions. Further south, there is approximately 112 km$^2$ close to the city of Guolimim with high APRHOS potential.

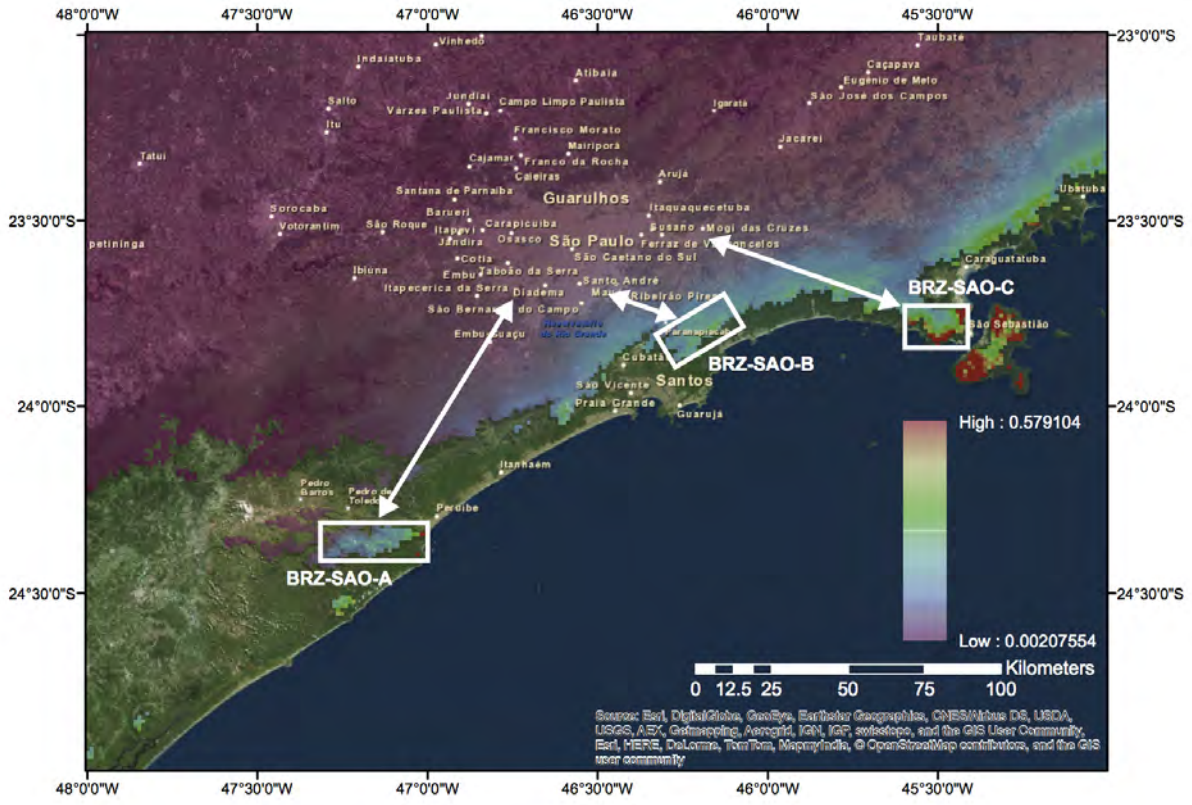


Figure 16: A-Index for topography near São Paulo, Brazil. Regions for potential APRHOS applications highlighted in white with distance to nearest major city, São Paulo, indicated by arrows.

In both cases, although the mountain ridges are far from the coast (¿10 $km$), one possibility would be to harness the excellent wind at the top of these ridges using wind turbines. These could then be used to power not only the pumping of water up to the APHROS storage lakes, but they could also provide additional electricity that could be sent via electric power transmission lines to regions where it is needed most. Additionally, the water in the APRHOS storage lakes can still be used to generate electricity and freshwater for the coastal regions as well as east to low lying desert regions. The freshwater routed to the east could be used for irrigation while the salt and minerals from the brine produced could be harvested through the use of evaporation ponds. This case study of regions in Morocco demonstrate other variations on how the APHROS system can be configured.

Table 7: Energy potential of APRHOS in regions in Morocco

| **Region** | **Head (m)** | **Surface area (km$^2$)** | **Distance from coast (km)** | **A-Index** | **Nearest major city (NMC)** | **Distance to to NMC** | **Energy potential (GWh/cycle)** |
|---|---|---|---|---|---|---|---|
| MOR-AGA-A | 687 | 292 | 13 | 0.053 | Agadir | 3.9 | 13503 |
| MOR-GUO-A | 582 | 112 | 13 | 0.044 | Guolimim | 27 | 4380 |

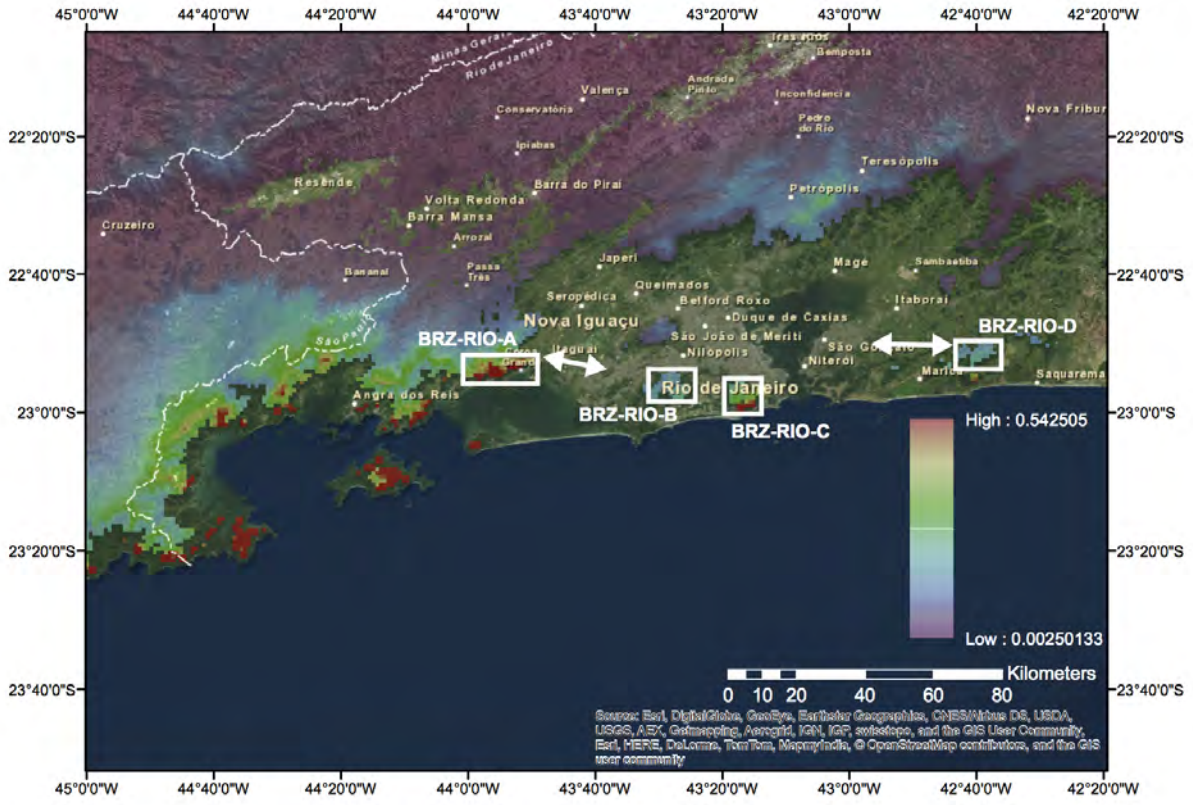


Figure 17: A-Index for topography near Rio de Janeiro, Brazil. Regions for potential APRHOS applications highlighted in white with distance to nearest major city, Rio de Janeiro, indicated by arrows.

## 3.8 Middle East

The Middle East has great natural resources of many forms, including a rich history of great civilizations whose citizens accomplished amazing feats of civil engineering. Unfortunately now as in the past, water scarcity has often been a source of contention between peoples. Presently water shortages can be relieved by RO plants, but this currently mostly involves burning hydrocarbons to generate the power required. Fortunately there are many excellent IPHRO system sites in the Middle East as well as the will and means in many countries to plan and create for the future.

### 3.8.1 Northern Red Sea (Egypt, Israel, and Jordan)

The region around the northern Red Sea along the borders of Egypt, Israel, and Jordan is also a region with large IPHRO potential. The mountains close to the coast of the Red Sea and the great need for freshwater in the bordering countries makes this an ideal site to investigate. Figure 19 highlights the regions around the cities of Taba in Egypt, Eilat in Israel, and Aqaba in Jordan that have high A-Indices. As can be seen from the figure, for each of the major cities in the region, there are corresponding areas that can be developed for IPHROS. Table 8 summarizes these results.

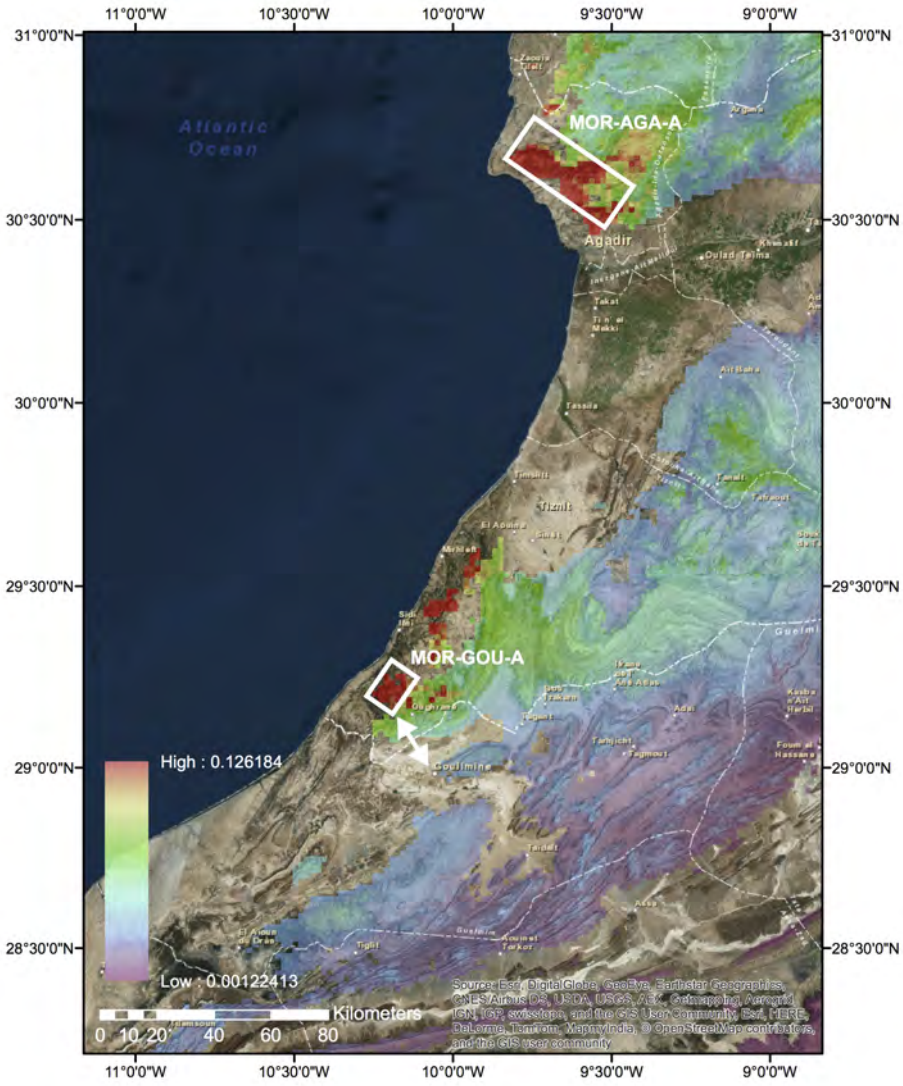


Figure 18: A-Index for topography of regions in eastern Morocco. Regions for potential APRHOS applications highlighted in white with distance to nearest major city, indicated by arrows.

For the case of Taba, Egypt, the region highlighted by REDSEA-A could provide enough power and freshwater for nearly 11 million people, while REDSEA-B could do the same for up to 3.45 million people in Eilat, Israel and REDSEA-C represents the opportunity to provide over 29 million people with power and freshwater in Aqaba, Jordan. It is important to note that the entire population of Israel is only 8 million people and that of Jordan is 7 million people, therefore if only a fraction of the areas highlighted are developed for APRHOS, they still present a great opportunity to provide both power and freshwater to a vast majority of local inhabitants. Given extreme drought in the region and migration of people from war torn regions, IPHRO systems have the potential to employ many and provide power and fresh water to enable formation of new stable

centers of civilization along the coasts.

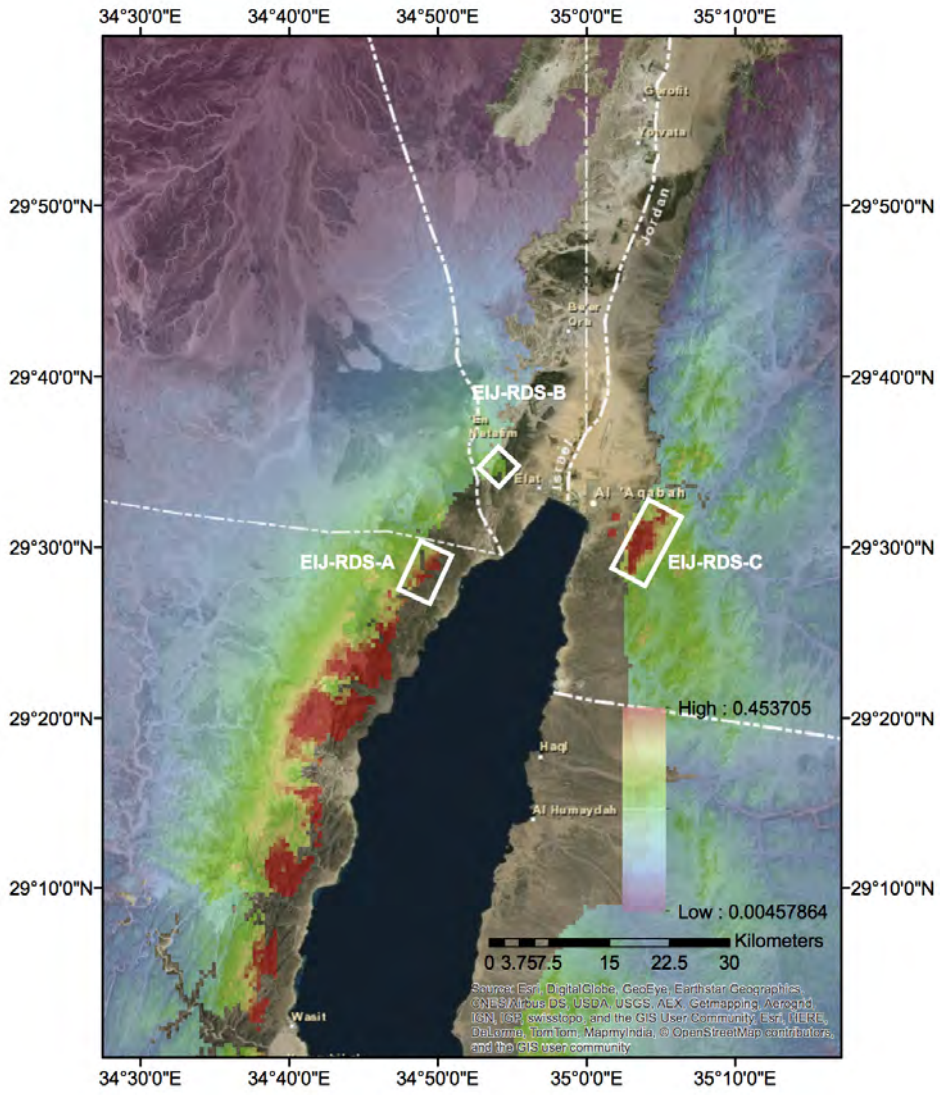


Figure 19: A-Index for topography of regions in the northern Red Sea. Regions for potential APRHOS applications highlighted in white. The closest city to the regions REDSEA-A, REDSEA-B, and REDSEA-C are Taba in Egypt, Eilat in Israel, and Aqaba in Jordan, respectively.

Table 8: Energy potential of APRHOS in regions around the northern Red Sea

| **Region** | **Head (m)** | **Surface area (km$^2$)** | **Distance from coast (km)** | **A-Index** | **Nearest major city (NMC)** | **Distance to to NMC** | **Energy potential (GWh/cycle)** |
|---|---|---|---|---|---|---|---|
| REDSEA-A | 573 | 12 | 5.5 | 0.105 | Taba | 6.67 | 13503 |
| REDSEA-B | 560 | 3.8 | 7.2 | 0.0.078 | Eilat | 3.62 | 4380 |
| REDSEA-C | 817 | 32 | 8 | 0.102 | Aqaba | 5.11 | 13503 |

### 3.8.2 Iran

The population of Iran has its greatest density around Tehran which is close to the Caspian sea, but the region is chronically short of water. Fortunately there is great IPHRO system potential here. This could also help catalyze the renewable energy industry and negate the need for nuclear power plants. This might trigger substantial investment interest from the international community and enable Iran to emerge as a leader in the region for sustainable development.

Iran, one of the founding members of OPEC, has the world's fourth largest proven crude oil reserves and the second largest proven natural gas reserves. Naturally, oil and gas have played a dominant role in the country's energy dynamics, though the combination of Iran's mountainous topography and IPHROS could catalyze development of a long term renewable and sustainable energy industry. Energy consumption in 2012 was roughly 278 billion kWh [11], with forecasts estimating a mean annual growth of 1.8% until 2018 [12].

The Tehran metropolitan area has a population of close to 14 million people, and serves as the nation's political and economic capital. Over the past two decades, pollution has progressed relatively unchecked, and the air quality of Tehran has reached alarmingly dangerous levels [13]. Furthermore, water scarcity has evolved to be a significant issue for the city, and the nation at large, with disruptions and cuts arising frequently [14]. Essentially, these environmental issues pose a national security problem. In light of these issues, renewable sources of energy may alleviate some of the environmental strains while supplanting carbon-emitting power plants.

The IPHROS potential of sites near the capital of Tehran is shown in Figure 20, with further details of highlighted regions in Table 9. The best sites for IPHROS are located over 100 km away from the edge of the city. Nested between the Caspian Sea and the Tehran metropolis lies the Alborz mountain range, running along the coastline for 950 km [15]. Therefore may not be viable sources of direct freshwater via pipelines due to the significant amount of pipe losses across such long distances, although water from the Owens valley in CA has long supplied Los Angeles from similar distances. Recent experience gained by Chinese engineers building a canal from the south of China to the north could perhaps be applied here. Thus it is envisioned that a combination of canals and tunnels could reasonably provide a means to deliver immense amounts of freshwater to the parched interior. Indeed, the combined potential of the regions represents a lake area of approximately 125 $km^2$ and could provide enough electricity for over 115 million people. This far exceeds the population of Tehran, for which IPHROS would require only about 15 $km^2$ of lake area.

To the south lies the Zagros mountain range spanning the west and south of the country, hugging the northern coast of the Persian Gulf. Several cities derive the entirety of their energy needs from the oil fields of this region; namely, Shiraz and Bushehr. There is tremendous potential in IPHROS sites meeting the energy and economic needs of this region. The well-ordered topography of this region is ideally suited for the development of IPHROS technology, and the close proximity of major city and industrial centers provide a strong consumer base. The oil and natural gas industry can provide further economic motivation for the development of IPHROS as freshwater is needed for processing.

To the south, the IPHROS potential near the city of Shiraz is shown in Figure 21. The highlighted region, detailed in Table 9, represents a lake area of 245 $km^2$, if fully developed. Again, the distance between the reservoir and city is too great ($\sim$ 200 km) for the system to directly pump freshwater to Shiraz, however IPHROS in this area could provide electricity for over 225 million people. With a population of approximately 1.5 million [16], a system of only 1.72 $km^2$ of lake area would be required to meet all of the electricity needs of the city.

Farther east, the IPHROS potential near the city of Bandar 'Abbas is depicted in Figure 21. The highlighted regions, detailed in Table 9, represent a total lake area of 183 $km^2$, if fully developed.

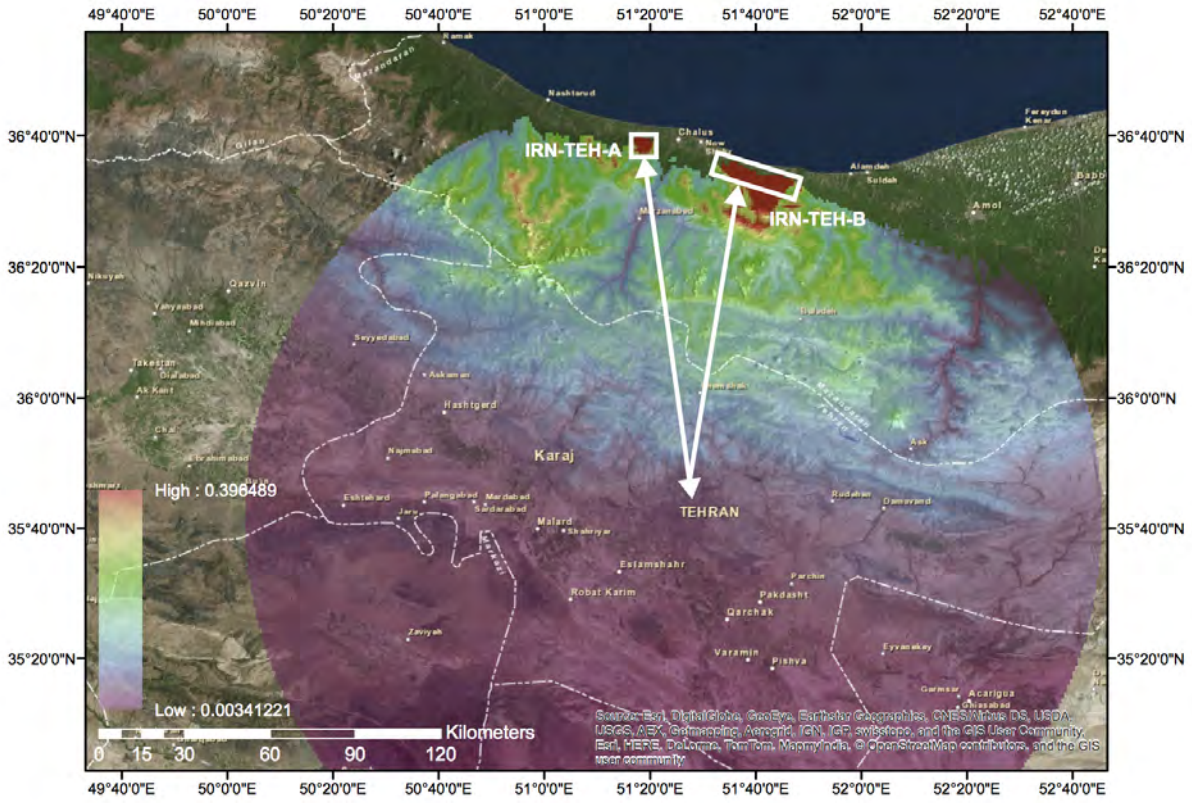


Figure 20: A-Index for topography of region near Tehran, Iran. Regions for potential APRHOS applications highlighted in white with distance to nearest major city, Tehran, indicated by arrows.

As before, with extremely long distances between the reservoir and the city, these regions may not be viable as a direct freshwater supply, however they could provide electricity for over 169 million people. With a population of only 435,000 [16], a system of only 0.46 km$^2$ of lake area would be required to meet all of the electricity needs of the city. The freshwater produced could irrigate farms which can provide produce for local and export consumption.

Given the challenging state of relations between Iran and much of the international community, any opportunity that can potentially build trust and enhance confidence should be considered and studied in detail with a potential fast track demonstration project undertaken to show that we can all really work together to create a better world for all. Joint-ventures of renewable energy projects perhaps can build on the relationships established by current nuclear power discussions between Iran and the P5+1. Not only might IPHROS projects engage the educated and talented workforce of Iran, but they could provide the government a means by which to focus national attention on sustainable energy and water production development. Indeed, if the IPHROS technology could be developed as imagined, there would simply be no need for nuclear power plants in the region.

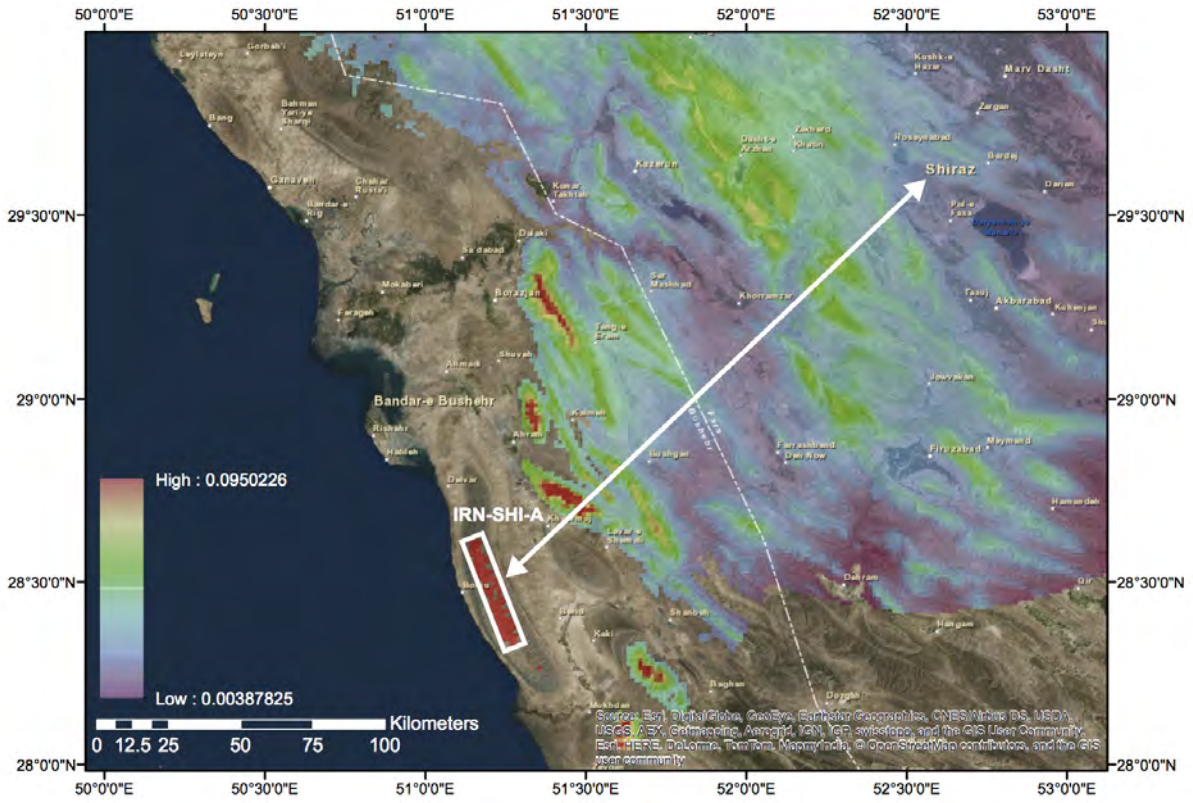


Figure 21: A-Index for topography of region near Shiraz, Iran. Regions for potential APRHOS applications highlighted in white with distance to nearest major city, Shiraz, indicated by arrows.

Table 9: Energy potential of APRHOS in regions in Iran

| Region | Head (m) | Surface area (km$^2$) | Distance from coast (km) | A-Index | Nearest major city (NMC) | Distance to to NMC | Energy potential (GWh/cycle) |
|---|---|---|---|---|---|---|---|
| IRN-TEH-A | 778 | 32 | 6.4 | 0.122 | Tehran | 132 | 1672 |
| IRN-TEH-B | 888 | 93 | 4.2 | 0.211 | Tehran | 100 | 5547 |
| IRN-SHI-A | 565 | 245 | 8.4 | 0.067 | Shiraz | 200 | 9297 |
| IRN-BAN-A | 645 | 75 | 5.9 | 0.110 | Bandar 'Abbas | 128 | 3240 |
| IRN-BAN-B | 730 | 109 | 9.3 | 0.078 | Bandar 'Abbas | 72 | 5339 |

### 3.8.3 United Arab Emirates

The United Arab Emirates (UAE), led by Khalifa bin Zayed bin Sultan Al Nahyan and other leaders within the UAE, has demonstrated a clear vision to plan for a renewable energy based future. For example, the Masdar Institute was created to develop renewable resource technologies and itself have a zero carbon footprint [17]. The total population of the UAE is about 15 million, with native Emiratis comprising just over 9 million [16]. The mountains west of Masafi have good IPHRO potential as shown in Figure 23. Indeed given likely great wind energy potential high in the mountains and the vast desert (and mountain) regions available for solar PV plants, the entire

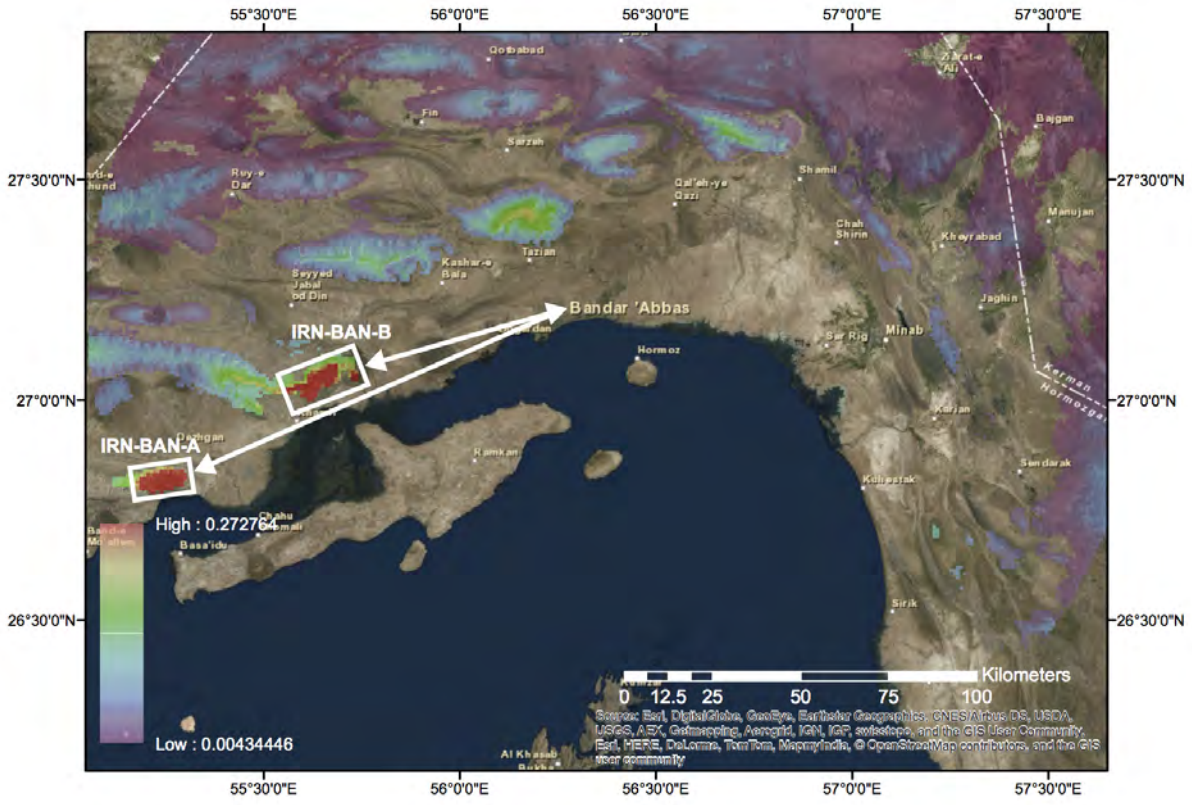


Figure 22: A-Index for topography of region near Bandar 'Abbas, Iran. Regions for potential APRHOS applications highlighted in white with distance to nearest major city, Bandar 'Abbas, indicated by arrows.

country could be powered and watered with renewables, thus obfuscating the need for the full build-out of nuclear power plants that are currently planned [18].

The IPHROS potential for the eastern United Arab Emirates is shown in Figure 23. Further detailed in Table 10, the highlighted regions represent a lake area of nearly 13.5 km$^2$. If fully developed, these regions could provide enough electricity and freshwater for 12.4 million people. If freshwater is the desired output of the system, this area could provide enough water for nearly 104 million people.

Table 10: Energy potential of APRHOS in regions in the United Arab Emirates

| **Region** | **Head (m)** | **Surface area (km$^2$)** | **Distance from coast (km)** | **A-Index** | **Nearest major city (NMC)** | **Distance to to NMC** | **Energy potential (GWh/cycle)** |
|---|---|---|---|---|---|---|---|
| UAE-ALF-A | 529 | 0.64 | 2.8 | 0.186 | Khor Fakkan | 2.7 | 23 |
| UAE-ALF-B | 619 | 12.8 | 8.5 | 0.073 | Fujairah | 7.3 | 533 |

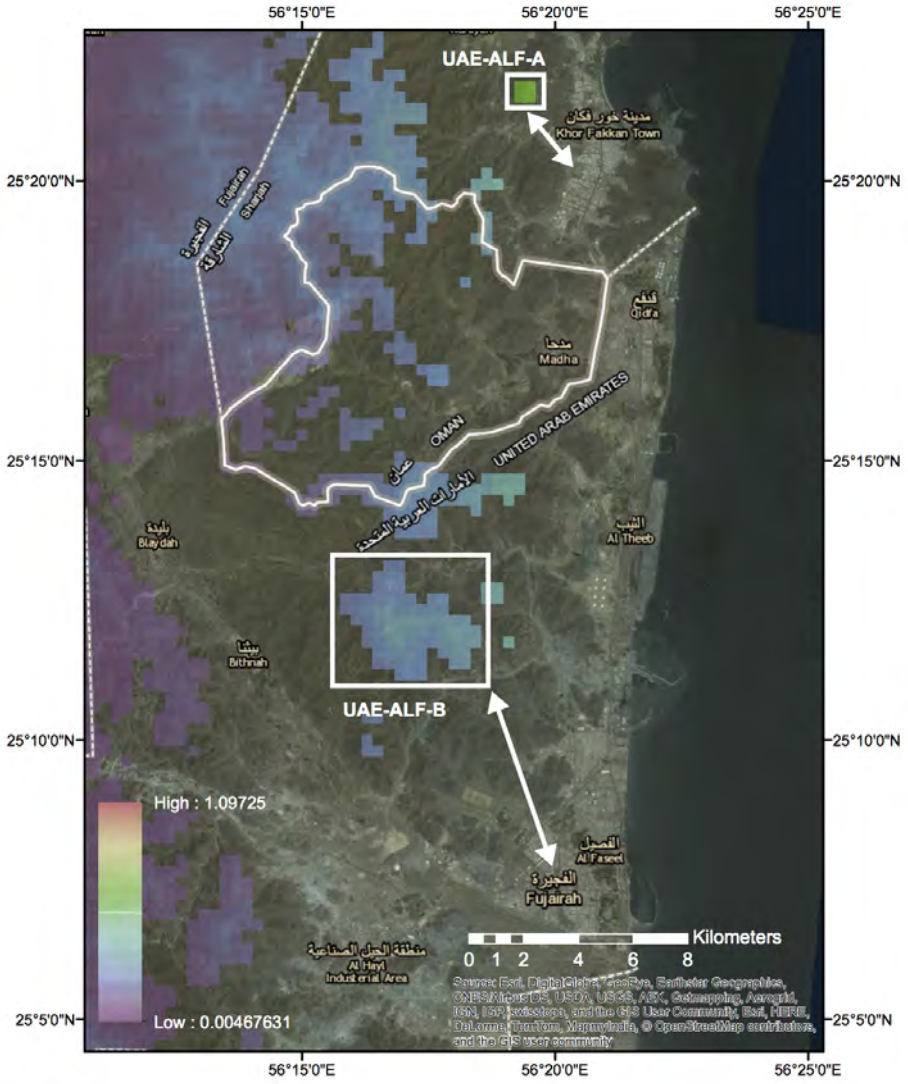


Figure 23: A-Index for topography of the eastern United Arab Emirates. Regions for potential APRHOS applications highlighted in white with distance to nearest major city indicated by arrows.

## 3.9 China

A canal from the south is currently under construction to transport water to the thirsty north [19]. This monumental feat of engineering, however, is seen by some as only a temporary fix for the north's long term water shortage challenges, and has displaced up to a million Chinese from their homes to make way for construction. To alleviate the environmental and social impact of such a project, perhaps it would be better to develop an APHRO system on the coast in conjunction with offshore wind turbines as renewable energy sources. Additionally, there are discussions underway regarding the shipment of water to Kinmen (Taiwanese island two kilometers off the coast of China)

via pipelines [20]. Figure 24 shows an image of the region and the potential lake areas in the regions of Ningde and Fuzhou. Figures 25 and 26 shows these regions in more detail.

The regions highlighted Figures 25 and 26 are further detailed in Table 11. The areas highlighted represent a total lake area of about 118 km$^2$. Using the provided spreadsheet, this means these regions could provide power and fresh water for about 108 million people. The amount of water used for desalination is only 4.7% of the total pumped to the lake.

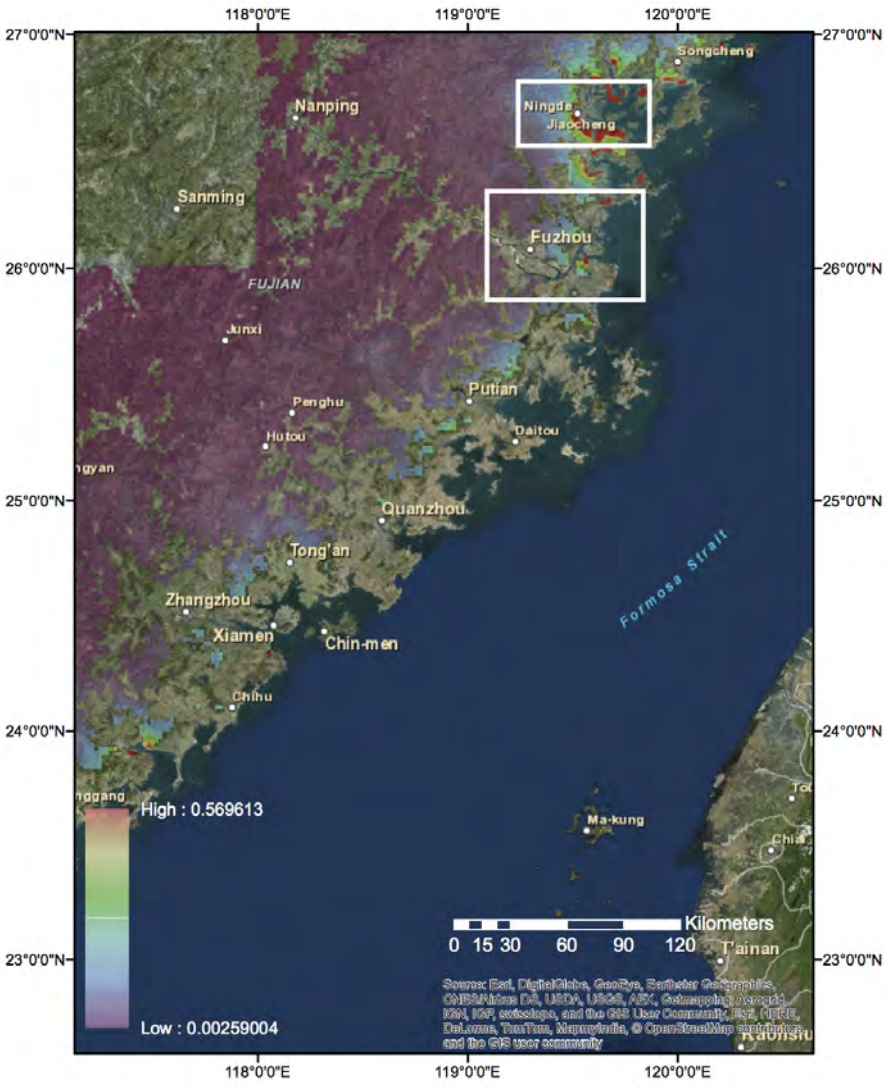


Figure 24: A-Index for topography in Eastern China.

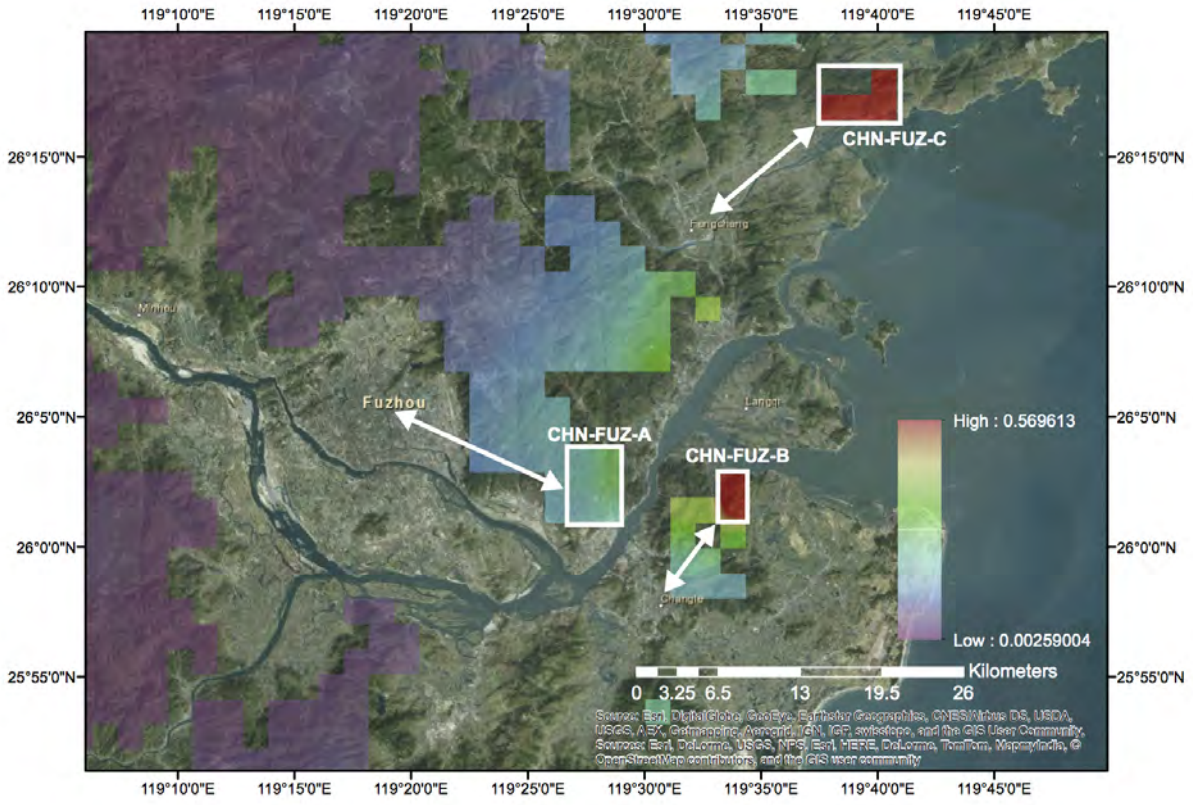


Figure 25: A-Index for topography near Fuzhuo, China. Regions for potential APRHOS applications highlighted in white with distance to nearest major city indicated by arrows.

Table 11: Energy potential of APRHOS in regions in Eastern China

| Region | Head (m) | Surface area (km$^2$) | Distance from coast (km) | A-Index | Nearest major city (NMC) | Distance to to NMC | Energy potential (GWh/cycle) |
|---|---|---|---|---|---|---|---|
| CHN-FUZ-A | 548 | 23 | 7.3 | 0.075 | Fuzhou | 17 | 839 |
| CHN-FUZ-B | 534 | 6.7 | 3.0 | 0.178 | Changle | 8.0 | 241 |
| CHN-FUZ-C | 507 | 15 | 1.9 | 0.267 | Fengcheng | 14 | 514 |
| CHN-NIN-A | 668 | 38 | 3.5 | 0.194 | Ningde | 1.5 | 1696 |
| CHN-NIN-B | 604 | 35 | 3.8 | 0.158 | Ningde | 13 | 1434 |

# 4 Detailed economic analysis case study – Southern California

The first order analysis indicates feasibility of the approach, but a much more detailed analysis is warranted as part of any significant effort to move forward. As an example, here we consider a high-resolution analysis of the economics of an exemplary project in Southern California. Such detailed analysis helps to understand the effect of actual market prices, regulatory obligations, system configuration, capital and operating cost on the project's technical and financial performance. For

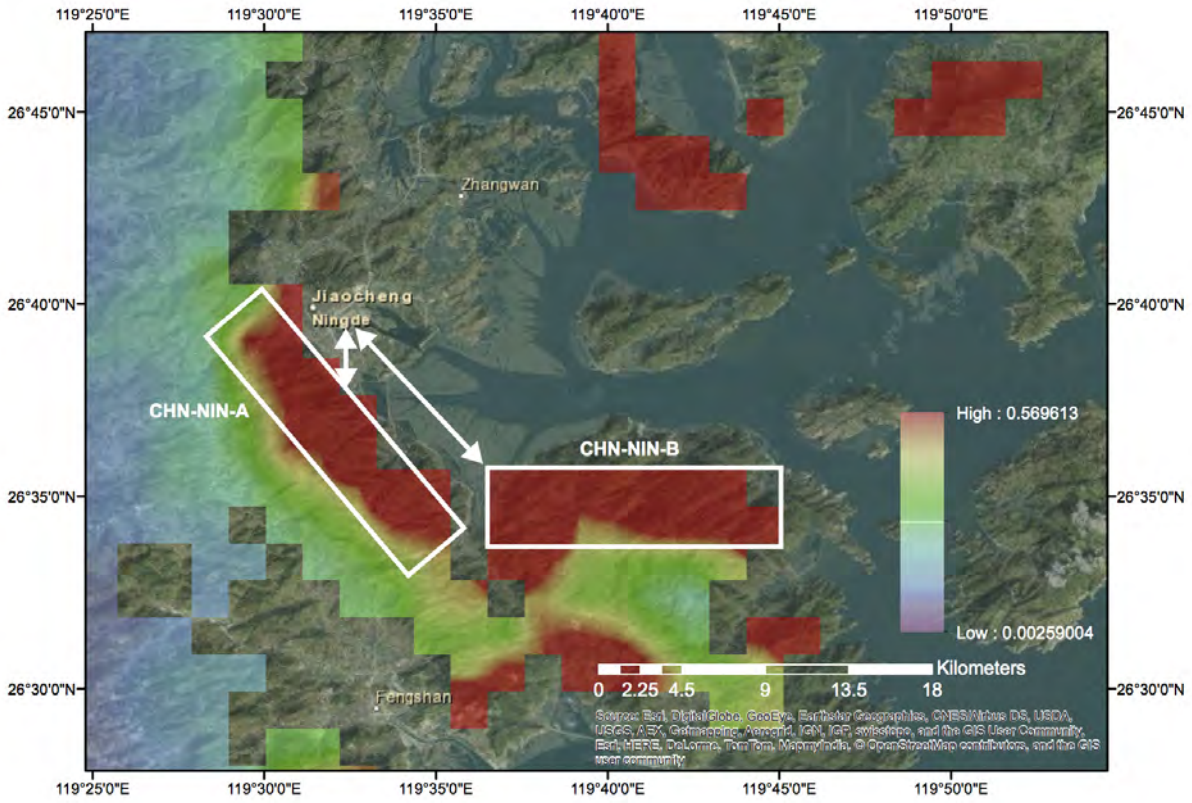


Figure 26: A-Index for topography near Ningde, China. Regions for potential APRHOS applications highlighted in white with distance to nearest major city, Ningde, indicated by arrows.

the purpose of this analysis, we use a commercial energy storage analysis software ESWare$^{TM}$[3]. ESWare was developed by 24M Technologies, Inc. to study the techno-economic performance of energy storage systems (ESSs) in various applications and combined sets of applications. ESWare is a chronological dispatch simulator that calculates and enacts the profit maximizing dispatch strategy of an energy storage system at high resolution. Realistic energy and capacity charge scenarios, incentive schemes, market prices, capital cost and operating costs and energy storage wear and tear models are fed to a constrained non-linear programming engine for dispatch optimization; an economic calculator produces detailed financial performance analysis and cash-flow projections.

In our baseline scenario, assume that a Load Serving Entity (LSE) in the Los Angeles area has to purchase energy and capacity to supply customers in its service area. Wholesale energy prices from the trading hub SP15 from 2014 are downloaded from the California Independent System Operator (CAISO) website OASIS. Such prices vary from a minimum of \$0.0143kWh to a maximum of \$0.165/kWh with a yearly average of \$0.0465kWh. In order to account for capacity charges, we assume an equivalent monthly cost of \$10/kW-month: the peak load of each month is

[3]The software ESWare$^{TM}$ is not publicly available at this time. The authors remain available for clarifications and can be reached at mferrara@alum.mit.edu

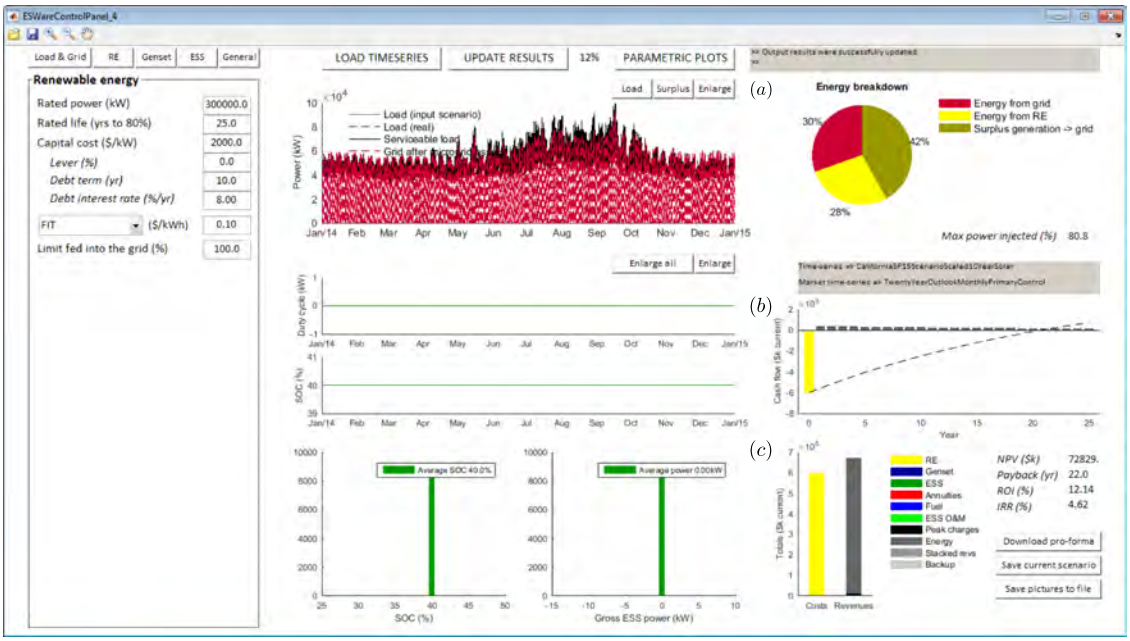


Figure 27: Scenario 1

multiplied by this number to calculate the cost of generation and Transmission and Distribution (T&D) capacity. While this may not exactly match the capacity costing method of a LSE in the area under study, it is nevertheless representative. The load profile is also downloaded from OASIS; in particular, the load from the Eastern Central Transmission Access Charge (TAC) area is used, after rescaling to 100MW summer peak load, to represent a smaller pocket of load. Finally, the solar resource is modeled by calculating a ten year average of yearly time-series from the National Solar Resource Database (NSRDB) as measured at the Los Angeles International Airport. Any excess solar generation can be sold under a Power Purchase Agreement (PPA) at a fixed price \$0.10/kWh. All financial analysis assumes a contract term of 25 years, no incentives and is based on full equity investment.

In a first scenario shown in Figure 27, we assume that a large PV plant of 300MW of peak generating capacity is used to supply part of the LSE load. Solar generation substantially exceeds the local load requirements, in particular in shoulder months, however this excess generation can be monetized at a fixed price of \$0.10/kWh. The combined economics of offsetting peak power prices and selling the excess generation at a favorable PPA, as shown in the energy breakdown ($a$), make for a profitable investment ($b$), albeit not at a level of internal return that would interest many investors. It should be noted that no tax credit was assumed in this analysis and that the PV plant is entirely financed with equity.

Next, a Pumped Hydro Energy Storage System (ESS) is added (Figure 28). The first ESS configuration tested is an ideal 4 hour system. Although not necessarily the optimal configuration from a financial standpoint, it is used to demonstrate renewable and grid energy arbitrage. The ESS will act to minimize energy cost and peak demand charges by flattening the daily net load, which is the difference between the daily load and the renewable generation. The entity of PPA sales diminish ($a$), but the combination of PV and ESS is very effective at minimizing peak demand charges and returns are similar to the case in Figure 27 ($b$). The ESS is dispatched daily in such a way as to minimize the total energy cost, while complying with power and energy constraints as well as with the final State of Charge (SOC) condition of center of Depth of Discharge (DoD). Keep

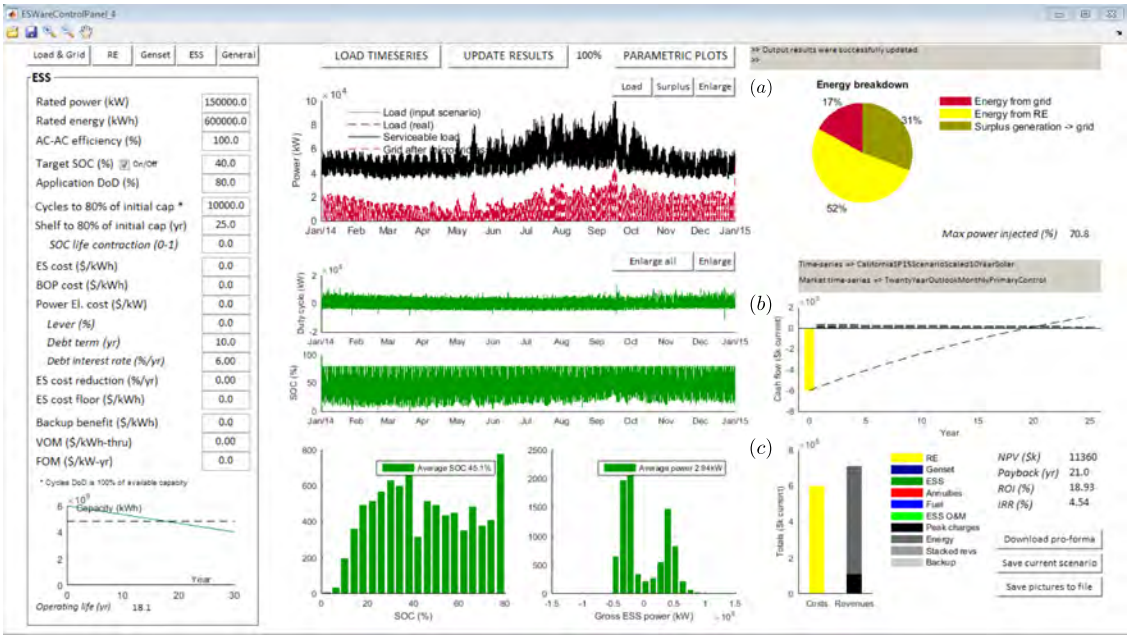


Figure 28: Scenario 2

in mind that the cost of the PS is assumed to be zero for the moment. When the actual capital and operating costs of the PS system are added to the problem, the returns become substantially negative. We must then consider additional value streams, such as the fresh water output of a collocated RO plant, and establish whether the additional benefits can offset the additional costs of such a plant.

Figure 29 shows a case study where a RO plant is added to the PS system. The assumption is that 20% of the return water flow from the PS system is diverted into the RO plant. The capital and operating costs and the round-trip efficiency inputs in ESWare are updated to account for the additional losses, costs and benefits of the RO plant. The system economics improves with respect to the PS alone, however returns are still negative $(b, c)$.

Finally, we consider an alternative scenario of higher energy prices ($0.05/kWh-$0.30/kWh averaging $0.104/kWh over a year) and a higher capacity charge of $20/kW-mo, with the ESS system sized at 100 MW and 600 MWh, and 50% of the ESS water passing through the RO plant. The basic economics improves greatly $(b, c)$ as shown in Figure 30: returns are now higher than the PV alone in similar conditions and the rates of return meet the hurdle rate of infrastructure funds.

This study shows that a comprehensive parametric analysis is required to understand conditions for economic justification of an APHRO system, including considering the time-structure and the long term forecasts for power and fresh water prices. It is also apparent that some degree of grid access and central infrastructure is helpful to achieve high availability and a low cost of energy.

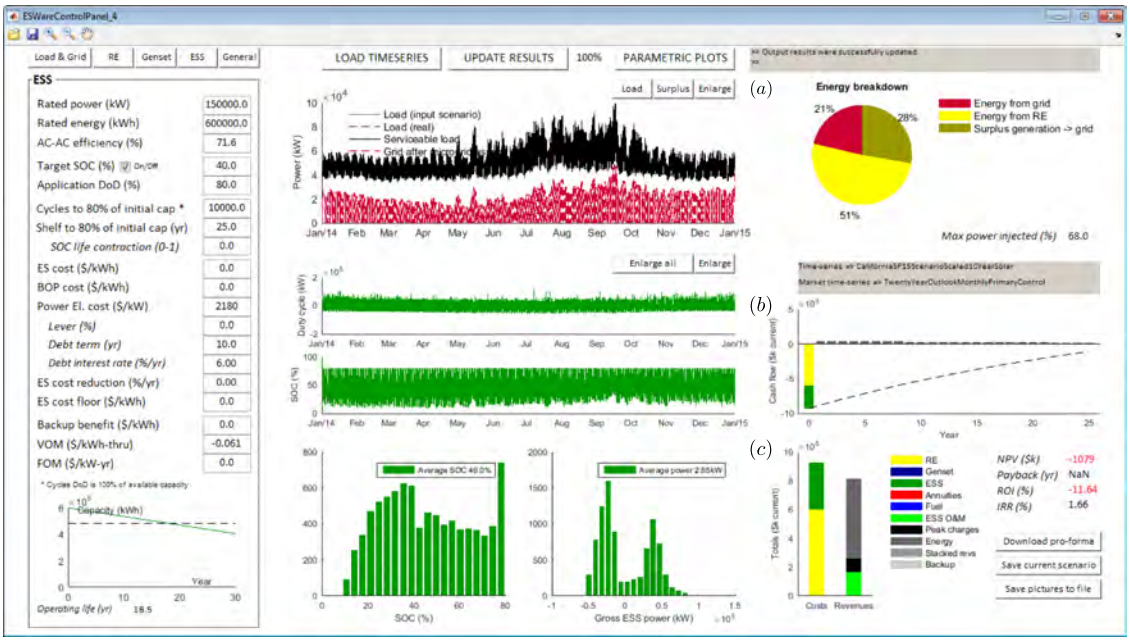


Figure 29: Characteristics of a system with PV renewable power generation, pumped hydro energy storage system, and collocated reverse osmosis plant

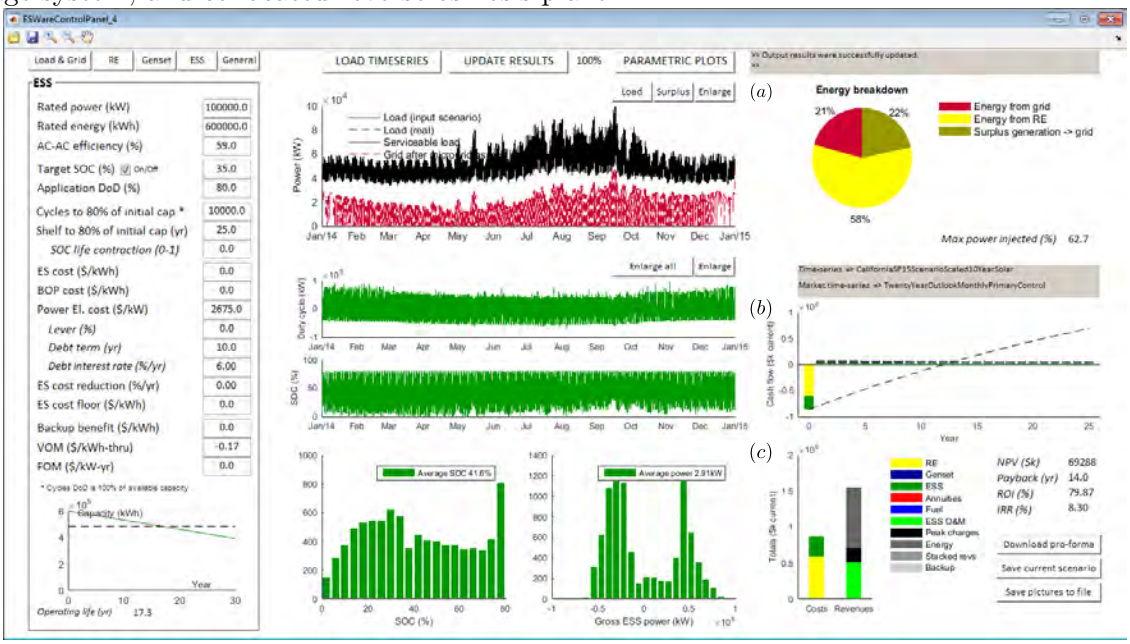


Figure 30: Characteristics of a system with PV renewable power generation, pumped hydro energy storage system, and collocated reverse osmosis plant operated in a more aggressive water production mode with higher energy prices.

# 5 Environmental and Cultural Considerations

Many sites are remote and large enough, such as in Chile, so placement of an APHRO system could be easily accommodated as a form of sustainable development. Other regions are in the vicinity of populated areas, but the mountains for lake placement are very dry and scarcely used by people. Although the voices of a few may say humans have encroached enough, prolonged droughts are having a devastating effect on local flora and fauna so a compromise might be to set aside a value such as 10% of the freshwater generated to be pumped back up to replenish mountain streams and ponds that used to exist before the drought in support of wildlife.

In other regions, such as Hawaii, there may be cultural objections to APHRO systems because the lakes might cover ancestral burial grounds. Once again, balance and compromise needs to be considered. Which causes greater concern for the spirits of our ancestors: the continued destruction of the planet by taking all the water from a region so wildlife suffer while we burn hydrocarbons for electricity and poison the atmosphere, or knowing that a lake atop their bones brings environmentally sustainable relief to all creatures? A path forward here would be to introduce these ideas for discussion and debate at all levels from grade school to community meetings.

Another environmental issue to be studied is what is the effect of daily alternating loading on the geology from the great weight of water daily being cycled to and from the high altitude reservoir? Unlike injection of water deep into the earth for geothermal power or fracking, where there are indications that earthquakes are being triggered, the loads applied by the lake cycling are on top of the strata and are greatly diffused by the time they would reach any slip planes. Seismic data from the Yanbaru facility, as well as other current pumped hydro locations, needs to be carefully studied. In addition, the remote site Valhalla Inc. is developing in Chile could yield data early on, and thus the site should be well instrumented to provide data on geologic motions correlated to the pumping cycles.

# 6 Advancements in Renewables and Reverse Osmosis Systems

The prices of renewables assumed above are thought to be conservative, and still yield acceptable return on investment periods. History would indicate that further advances in technology not only will occur, they will occur faster when there is a clear need and market pull. For example, in just a few short years solar cells have become ever more efficient and lower cost, for reasons including the discovery of new materials such as perovskite based solar cells [21]. Increases in efficiency and accompanying decreases in effective cost/kW can thus be expected as initial “must have ASAP” APHRO systems are created and their efficacy becomes apparent.

Similarly, adoption of the APHROS technology would help catalyze reduction in reverse osmosis costs. For example, Israel’s needs for fresh water led to the Sorek desalination plant being commissioned with larger pipes for the RO membranes, and the cost of produced water dropped dramatically [22].

History has shown that what is expensive and infeasible today, often becomes economical and commonplace tomorrow!

# 7 Further Research

- Valhalla’s site in Chile should be considered as an international study center for APHROs concept, from effect of cyclic loading on coastal geology to how best to operate the RO plant, and economic activity that results from availability of power and fresh water in a desert region

- Cost analysis of deeper lake with smaller footprint, but then the sides of the lake may need more reinforcement, just like a swimming pool; hence what is the trade off and for a given region how can the lake design be optimized to minimize costs?

# 8 Facing the Sun: A Student Foundation for the Clean Energy Economy

## 8.1 Summary

President Obama believes that giving students more "hands-on" opportunities is critical to getting more boys and girls excited about STEM education. As he said at the launch of his "Educate to Innovate" initiative, "I want us all to think about new and creative ways to engage young people in science and engineering, whether it's science festivals, robotics competitions, fairs that encourage young people to create and build and inventto be makers of things, not just consumers of things."

One possible initiative that could help meet this goal would be to increase the number of students that are involved in the design, installation and maintenance of solar energy systems for their schools. This would allow students to make a lasting contribution to accelerating Americas adoption of clean sources of energy, and to learn about a variety of STEM subjects in the process. In addition, because the intent is to have the systems continue to function even after the students graduate, the total amount of renewable energy produced would grow rapidly; and students would learn about designing and making things that last.

## 8.2 Hypothesis

Photovoltaic (PV) systems have great promise because they can be incrementally installed just about anywhere, and hence could steadily increase the amount of solar power provided and over time significantly reduce the use of fossil fuels used to generate electricity.

- *Cost:* the cost of PV panels and their installation is decreasing and will continue to decrease, a goal that the Department of Energy is pursuing through its SunShot initiative.

- *Energy storage:* with the increasing popularity of hybrid and electric vehicles, there will be an increase in the availability of batteries from cars at their end-of-life, which are still good enough for residential, commercial/industrial, and military energy storage, such as in the DOD's ESTCP Installation Energy Test Bed Initiative (`http://www.serdp.org/Featured-Initiatives/Installation-Energy`).

- *Maintenance:* Pollen, dust, salt there are many contaminants that can slowly coat the surfaces of panels and reduce their effectiveness. Cleaning is expensive especially in terms of water consumption, and labor in high labor cost regions. Herein lies a great opportunity in terms of design and also realization: There are a plethora of ideas that one can imagine to address the cleaning opportunity and there is also a need for engineering and renewable energy education.

To help catalyze a hands-on design and manufacturing curricula, schools could offer as a major term project "PV Panel Deployment". Teams of students would be given the resources and training needed to design, build, deploy, and test a solar energy system. Teams could compete to deploy panels that operate successfully and generate the most electricity over a period of time for minimum cost; engineering and business skills will be also thus be required to be truly successful. This would

include students are allowed to hack other students systems to turn them away from the sun, so they better have great IT security in place!

Unsuccessful systems would serve as learning examples and materials would be reused. High-performing systems would be kept in operation for the useful life of the panels . This can also help teach design for assembly (DFA), design for manufacturing (DFM), design for recycling (DFR), and product lifecycle management (PLM) skills to the students. These skills and techniques are especially valuable to US students, workers, and businesses not only from environmental and cost-efficiency standpoints but also for reducing the costs and balance of trade deficits for imported materials and energy systems. N years from deploying their system, students resumes can point to their still functioning system as compelling evidence of their engineering prowess.

This project could help accomplish a number of important goals:

1. As the design challenge spreads to more and more schools, the number of PV systems deployed (and remaining in operation) will increase.
2. Materials from other hands-on design events (e.g., FIRST) could be re-purposed (the best form of recycling).
3. More and more students who understand energy, conservation, and PV systems will graduate and hence will help to further innovate with regard to installation and operation of PV systems.
4. Better systems will evolve and new companies will be launched to capitalize on the best ideas.
   (a) Hardware, services, and software (including cyber secure systems) will all benefit.
   (b) This further improves the US skills gap, energy independence, and US exports of technical goods and services, and the US trade deficit.
5. This effort could strengthen the partnership between schools and energy companies and lead to dynamic AP engineering and manufacturing courses.
6. Other aspects of education in schools will benefit if students creating their machines make up homework problems (and solutions) motivated by their design and development work. These problems get tested (and evolved) by their peers and then can be uploaded to a national database.
   (a) Students could write apps to mine the database to collate for teachers to use in their classes problems and suggested resources for solving the problems.
   (b) Students will develop a sense of pride, ownership and see and personally feel that that Yes We Can take control of our own destiny.
   (c) The skills and experiences gained by the students will be great for their college applications and job applications. This is especially true in the modern multi-media era, where pictures and videos of their projects can bring better visualization and thus more concrete realization of the students' achievements and potential.
7. By starting the program in the poorest schools and seeking help of skilled veterans as coaches and mentors, discipline, pride, and a full range of engineering and manufacturing skills can be developed.
   (a) Local company support will be sought, especially in the form of guaranteed good summer jobs for students who are actively engaged in the program.

## 8.3 By the Numbers

These "back of the envelope" calculations show what might be accomplished in the near future:

| Assume a team consists of one each 9, 10, 11, and 12th grader | |
|---|---|
| Potential number of teams | 3,738,831 |
| Watts per panel | 250 |
| Number of panels | 2 |
| Cost per panel | $265.00 |
| Integration cost multiplier, cost | 2 |
| Mechanical system multiplier, cost | 3 |
| Total cost | $3,180.00 |
| Cost per installed watt average power | $42.40 |
| Cost per installed watt peak power | $6.36 |
| 24/7 capacity factor | 15% |
| Average power (W) | 75 |
| Peak power (W) | 500 |

The cumulative power that could be deployed nationwide is considerable:

| Total installed power (MW) | | | |
|---|---|---|---|
| Year | % Seniors | 24/7 average | Peak |
| 2015 | 5% | 14 | 93 |
| 2016 | 10% | 42 | 280 |
| 2017 | 15% | 84 | 561 |
| 2018 | 20% | 140 | 935 |
| 2019 | 25% | 210 | 1402 |
| 2020 | 30% | 294 | 1963 |

## References

[1] R. B. Schainker. Executive overview: energy storage options for a sustainable energy future. In *Power Engineering Society General Meeting, 2004. IEEE*, pages 2309–2314. IEEE, 2004.

[2] W. L. Kahrl. *Water and Power: The Conflict over Los Angeles' Water Supply in the Owens Valley*. University of California Press, 1982.

[3] C. Mulholland. *William Mulholland and the Rise of Los Angeles*. University of California Press, 2000.

[4] A. P. Williams, R. Seager, J. T. Abatzoglou, B. I. Cook, J. E. Smerdon, and Edward R. Cook. Contribution of anthropogenic warming to california drought during 2012–2014. *Geophysical Research Letters*, 2015.

[5] S. Jenkins, J. Paduan, P. Roberts, D. Schlenk, and J. Weiss. Management of Brine Discharges to Coastal Waters: Recommendations of a Science Advisory Panel. Technical Report 692, Costa Mesa: Southern California Costa Water Research Project, March 2012.

[6] United States Census Bureau. Annual Estimates of the Resident Population: April 1, 2010 to July 1, 2014, 2010.

[7] Secretara de Desarrollo Social. Catlogo de Localidades, 2010.

[8] Instituto Nacional de Estadsticas. Census, 2012.

[9] Brazilian Institute of Geography and Statistics. 2013 population estimates, 2013.

[10] U.S. Central Intelligence Agency. Brazil Temperature and Precipitation Map, 1977.

[11] U.S. Energy Information Administration. Iran, 2014.

[12] Hossein A., Yazdan G. F., and Ehsan A. G. Energy consumption in Iran with Bayesian approach 1. *OPEC Energy Review*, 36(4):444–455, dec 2012.

[13] T. Erdbrink. Annual buildup of air pollution chokes Tehran. *The New York Times*, Jan. 2013.

[14] J. Rezaian. Iran's water crisis the product of decades of bad planning. *The New York Times*, July 2014.

[15] M. Ghorbani. *The Economic Geology of Iran*. Springer Netherlands, 2013.

[16] United Nations Statistics Division, 2015.

[17] T. Heap. Masdar: Abu Dhabi's carbon-neutral city. *BBC News*, March 2010.

[18] E. Dyck and A. Evrensel. From Consideration to Construction: The United Arab Emirates' Journey to Nuclear Power. *IAEA Department of Nuclear Energy*, Feb 2015.

[19] J. Kaiman. Chinas water diversion project starts to flow to Beijing. *The Guardian*, Dec. 2014.

[20] Kinmen. The Politics of Water: Peace pipe. *The Economist*, May 2015.

[21] D. W. deQuilettes, S. M. Vorpahl, S. D. Stranks, H. Nagaoka, G. E. Eperon, M. E. Ziffer, H. J. Snaith, and D. S. Ginger. Impact of microstructure on local carrier lifetime in perovskite solar cells. *Science*, 348(6235):683–686, apr 2015.

[22] D. Talbot. Megascale Desalination: The worlds largest and cheapest reverse-osmosis desalination plant is up and running in Israel. *MIT Technology Review*, May 2015.